1067

NATIONAL ADVISORY COMMITTEE FOR AERONAUTICS

TECHNICAL NOTE

No. 1067

COMPARISON OF SEVERAL METHODS OF PREDICTING THE PRESSURE LOSS AT ALTITUDE ACROSS A BAFFLED AIRCRAFT-ENGINE CYLINDER

By Joseph Neustein and Louis J. Schafer, Jr.

Aircraft Engine Research Laboratory
Cleveland, Ohio

PROPERTY FAIRCHILD
ENGINEERING LIBRARY

Washington
May 1946

NATIONAL ADVISORY COMMITTEE FOR AERONAUTICS

TECHNICAL NOTE NO. 1067

COMPARISON OF SEVERAL METHODS OF PREDICTING THE PRESSURE LOSS AT ALTITUDE ACROSS A BAFFLED AIRCRAFT-ENGINE CYLINDER

By Joseph Neustein and Louis J. Schafer, Jr.

SUMMARY

Several methods of predicting the compressible-flow pressure loss across a baffled aircraft-engine cylinder were analytically related and were experimentally investigated on a typical air-cooled aircraft-engine cylinder. Tests with and without heat transfer covered a wide range of cooling-air flows and simulated altitudes from sea level to 40,000 feet.

Both the analysis and the test results showed that the method based on the density determined by the static pressure and the stagnation temperature at the baffle exit gave results comparable with those obtained from methods derived by one-dimensional flow theory. The method based on a characteristic Mach number, although related analytically to one-dimensional flow theory, was found impractical in the present tests because of the difficulty encountered in defining the proper characteristic state of the cooling air.

Although the cylinder-baffle resistance coefficient determined by the density method was consistent for a wide range of heat-transfer values, a distinct difference was observed between the values with and without heat transfer that could not be explained by one-dimensional flow theory. Accurate predictions of altitude pressure loss can apparently be made by these methods provided that they are based on the results of sea-level tests with heat transfer.

INTRODUCTION

The high operating altitudes of both military and commercial aircraft have greatly increased the severity of the engine air-cooling problem. The decrease of the density of the air with increased altitude necessitates the handling of a greater volume of air at higher velocities and, as a result, the flow of cooling-air within the fin passages attains high Mach numbers and a large decrease in the cooling-air density occurs across the engine. The pressure loss increases

with Mach number and consequently a greater pressure drop is needed to force a given weight of cooling air across the engine at high altitudes than would be required for the same weight flow of air at lower altitudes. This additional pressure loss, which is a function of Mach number, constitutes the compressibility effect and becomes a serious factor at high altitudes and high rates of heat transfer. It is important therefore to include the effect of Mach number in the prediction of cooling-air pressure-drop requirements at altitude.

Several methods of eliminating the compressibility effects have been proposed (references 1 to 5). In references 1 and 3 the air flow is assumed to be one-dimensional and two different solutions for determining the pressure drop are obtained. In references 2, 4, and 5, empirical solutions are presented. Each of the foregoing methods is apparently independent, however, and their interrelation has not been established. The tests of reference 2, which were made with a section of a cylinder barrel and which showed that the best results would be obtained by using one of the empirical factors, represent only an idealized situation. Tests on an actual aircraft-engine cylinder are therefore necessary to examine more thoroughly the proposed solutions to the compressibility problem.

The present investigation was conducted at the Cleveland laboratory of the NACA to evaluate by experimental data several methods of making compressible-flow pressure-drop predictions and to relate each method analytically by means of one-dimensional flow theory. The experimental work was done on a typical air-cooled cylinder enclosed in an air duct and mounted on a crankcase. The tests consisted in varying over a wide range the cooling-air pressure drop across the cylinder at cooling-air conditions that corresponded to altitudes varying from sea level to 40,000 feet. The tests were made both without engine operation and with the engine operating at several powers to determine the effect of heat transfer on cooling-air pressure drop.

SYMBOLS

The symbols used in this report are:

A	area, square feet
α_1, α_2, β_1, β_2	coefficients in Maclaurin's series
$C_3 - a_3$	baffle-exit pressure-loss coefficient

$C_{D_{f_i}}$	friction-drag coefficient of fin-baffle passage
F	pressure-drop coefficient of fin-baffle passage (includes pressure change at baffle exit and is equal to $C_{D_{f_i}}$ when this pressure change is negligible)
c_p	specific heat of air at constant pressure, 0.24 Btu per pound per $^{\circ}F$
G	cooling-air mass flow based on baffle free-flow area, slugs per second per square foot
g	acceleration of gravity, 32.2 feet per second per second
H	heat dissipated from cylinder to cooling air, Btu per pound
J	mechanical equivalent of heat, 778 foot-pounds per Btu
K, C, m, n, S	experimental constants
L	length of fin-baffle passage, feet
M	Mach number
p	static pressure, pounds per square foot
q	dynamic pressure, pounds per square foot
R	universal gas constant
Re	Reynolds number
T	static air temperature, $^{\circ}R$
T_h	average cylinder-head temperature, $^{\circ}R$
T_m	average cooling-air temperature in fin-baffle passage, $(T_2 + T_3)/2$, $^{\circ}R$
T'	ratio of cooling-air stagnation temperature rise across fin-baffle passage to static cooling-air temperature at baffle inlet, $\left(T_{3_t} - T_{2_t}\right)/T_2$

V	cooling-air velocity, feet per second
W	cooling-air weight flow, pounds per second
X	distance along fin-baffle passage measured from baffle inlet, feet
γ	ratio of specific heats for air, 1.395
μ	cooling-air viscosity, pound-second per square foot
ρ	cooling-air density, slugs per cubic foot
θ_3	angle between radius drawn to rear of cylinder and radius drawn to pressure-measuring station at baffle exit
σ_{av}	ratio of average cooling-air density to Army standard sea-level density
Δp	pressure drop from front to rear of cylinder, pounds per square foot
ΔT	cooling-air stagnation temperature rise across cylinder, $^{\circ}F$

Subscripts:

t	cooling-air stagnation condition
s	cooling-air condition at sea level
i	cooling-air flow condition without heat
o, x	characteristic condition of cooling-air flow
1	upstream of cylinder
2	baffle inlet
3	baffle exit
4	downstream of cylinder
h	cylinder head
b	cylinder barrel

ANALYSIS

The flow of air across a heated cylinder-baffle combination may be considered in three subordinate processes: (a) the flow into the fin-baffle passage (entrance process), (b) the flow through the fin-baffle passage (baffle flow process), and (c) the flow from the fin-baffle passage into the free stream (exit process). The flow into the fin-baffle passage is composed of the acceleration from the main stream to the baffle inlet during which the air receives some heat from the fins along the forward portion of the cylinder and incurs some pressure drop due to the friction loss along the fins and to the formation of the velocity profile. Local flow separation from the baffle wall probably occurs just beyond the baffle inlet. The entrance process is considered to be complete when full flow within the fin-baffle passage has been reestablished, although the point where this process ends is not definite.

The flow through the fin-baffle passage may be compared with that occurring in a bent channel in which the width approaches the radius of curvature in magnitude. A secondary flow normal to the direction of the main flow develops and transports low-energy air toward the inside of the bend. The accumulation of the low-energy air results in separation from the cylinder wall, usually before the baffle outlet is encountered. Separation will seriously modify the surface-friction coefficients of the channel. The flow is further complicated by the heat-transfer processes and by the irregular fin-baffle passages. The rate of heat transfer and the air flow are related through the mechanics of the boundary layer. Furthermore, the air acceleration resulting from heat addition along the fin passage causes an additional pressure decrease along the channel.

The flow of air from the baffle passage into the space downstream of the cylinder consists in an abrupt expansion similar to that occurring for the flow through a channel of discontinuous cross section. Because of the separation of the flow within the baffle passage, the point at which the exit process begins is uncertain. It is known that little heat transfer takes place between the rear fins and the air leaving the baffle passage.

One-Dimensional Flow-Theory Methods

As a means of simplifying the analysis, the fin-baffle passages are assumed uniform in width and only the velocities in the main direction of flow are considered. The entrance process may then be assumed to consist in the addition of heat at constant pressure at the front of the cylinder and the isentropic expansion from the front

of the cylinder to the baffle entrance. The relation between the pressures at the front of the cylinder and at the baffle inlet can therefore be expressed

$$p_2 = p_{1_t}\left(1 + \frac{\gamma - 1}{2} M_2^2\right)^{\frac{-\gamma}{\gamma-1}} \tag{1a}$$

or, in terms of the mass flow of cooling air, equation (1a) gives

$$\frac{G^2}{p_{1_t}\rho_{1_t}} = \frac{2\gamma}{\gamma - 1}\left[1 - \left(\frac{p_2}{p_{1_t}}\right)^{\frac{\gamma-1}{\gamma}}\right]\left(\frac{p_2}{p_{1_t}}\right)^{\frac{2}{\gamma}} \tag{1b}$$

The flow process through the fin-baffle passage can be represented mathematically by the differential form of the momentum equation modified to include the effect of friction. The rate of pressure drop along the channel is

$$\frac{-dp}{\frac{d(X)}{L}} = F\frac{\rho V^2}{2} + \rho\frac{d}{\frac{d(X)}{L}}\frac{V^2}{2} \tag{2}$$

where the first term on the right side of the equation represents the local pressure drop resulting from surface friction and the second term represents that due to reaction resulting from the local change of air density. Because the equation is not an exact differential, it is necessary to make either an assumption regarding the manner in which the heat is added to the air along the path or else to determine the ratio dp/ρ from the first law of thermodynamics in order that the equation be integrable. Two assumptions regarding the manner in which the heat is added lead to simple solutions: (1) the heat is added to the cooling air uniformly along the path (reference 3), and (2) the heat is added so as to increase the local dynamic pressure uniformly along the path (reference 1).

For the first assumption equation (2) is integrated (reference 3) as

$$\log\left(\frac{p_3}{p_2}\right)^2 + \frac{p_2^2}{RGT_m}\left[1 - \left(\frac{p_3}{p_2}\right)^2\right] - \left[F + \frac{2(T_3 - T_2)}{T_m}\right] = 0 \tag{3}$$

in which the pressure ratio across the baffle passage p_3/p_2 is determined implicitly. The pressure drop from the main stream to the baffle exit is therefore

$$p_{1_t} - p_3 = p_{1_t}\left(1 - \frac{p_2}{p_{1_t}}\frac{p_3}{p_2}\right) \tag{4}$$

where p_2/p_{1_t} is obtained from equation (1b).

The second assumption leads to the equation (reference 2)

$$\frac{p_2 - p_3}{q_2} = \frac{C_{D_{f_i}}}{2}\left(\frac{\rho_2}{\rho_3} + 1\right) + 2\left(\frac{\rho_2}{\rho_3} - 1\right) \tag{5}$$

By use of the first law of thermodynamics, equation (2) may also be integrated to give the familiar energy equation

$$\frac{V_2^2}{2} + \frac{\gamma}{\gamma - 1}\frac{p_2}{\rho_2} + JgH = \frac{V_3^2}{2} + \frac{\gamma}{\gamma - 1}\frac{p_3}{\rho_3} \tag{6}$$

Equations (5) and (6) can then be solved simultaneously with the continuity equation to give (reference 2)

$$\frac{\rho_2}{\rho_3} = 1 + T' + \frac{\gamma - 1}{2}M_2^2\left\{1 - \left(\frac{\rho_2}{\rho_3}\right)^2 + \frac{2\gamma}{\gamma - 1}\frac{\rho_2}{\rho_3}\left[\frac{C_{D_{f_i}}}{4}\left(1 + \frac{\rho_2}{\rho_3}\right) + \frac{\rho_2}{\rho_3} - 1\right]\right\} \tag{7}$$

The density ratio from equation (7) when substituted in equation (5) yields the pressure drop across the baffle channel. The entire pressure drop is then obtained from equation (4).

Inasmuch as equations (3), (5), and (7) all originate from equation (2) and differ only in the assumption regarding the manner in which heat is added to the cooling air, it might be expected that the value of the pressure drop calculated under either assumption will be approximately the same. The method using assumption (1) offers the simpler solution.

In the case of an additional pressure recovery or loss at the baffle outlet, the pressure at the outlet and at the rear of the engine can be related (reference 2) by means of the momentum equation

$$\frac{p_3 - p_4}{q_3} = (C_3 - a_3) - 2\frac{A_3}{A_4}\sin\theta_3 + 2\left(\frac{A_3}{A_4}\right)^2\frac{\rho_3}{\rho_4} \tag{8}$$

The angle θ_3 is usually small and A_4 is usually large compared with A_3. The last two terms of equation (8) are consequently of secondary importance and may be neglected. Equation (8) then reduces to

$$\frac{p_3 - p_4}{q_3} = C_3 - a_3 \tag{9}$$

In most cases, however, when no attempt is made to recover any of the kinetic energy at the baffle outlet, the pressure change at the baffle exit may be entirely neglected.

The foregoing methods of predicting pressure drop at altitude are complex and therefore other more simple solutions have been offered. Two such solutions make use of: (1) the density at the baffle exit (references 2, 4, and 5), and (2) a characteristic Mach number determined by a pressure and a temperature that exist at some point along the flow path (reference 2).

Baffle-Exit Density Method

A dimensional analysis of the factors which affect the pressure drop indicates that the pressure-drop coefficient $\Delta p/q$ for a cylinder depends upon the Reynolds number, the Mach number, and the ratio of cooling-air-temperature rise across the cylinder to the inlet cooling-air temperature. The pressure-drop coefficient may be written as

$$\frac{\Delta p}{q} = f\left(\mathrm{Re},\ \mathrm{M},\ \frac{\Delta T}{T}\right)$$

or

$$\frac{2\rho\Delta p}{G^2} = f\left(\mathrm{Re},\ \mathrm{M},\ \frac{\Delta T}{T}\right)$$

The tests of reference 2 show that, if the pressure-drop coefficient is evaluated by means of the density at the baffle exit, the effect of Mach number will be reduced. A relation may be established between this simple baffle-exit density method and the more complicated one-dimensional flow theory. The development of this relation is established as follows:

If equations (1) and (5) are combined, the pressure drop from the free stream to the baffle outlet can be expressed

$$\Delta p = p_3 \left\{ \left(1 + \frac{\gamma}{2} M_3^2 \frac{\rho_3}{\rho_2} Q\right) \left[1 + \frac{\gamma - 1}{2} M_3^2 \frac{\rho_3}{\rho_2} \left(1 + \frac{\gamma}{2} M_3^2 \frac{\rho_3}{\rho_2} Q\right)\right]^{\frac{\gamma}{\gamma-1}} - 1 \right\} \tag{10}$$

where

$$Q = C_{D_{f_i}} + \left(\frac{C_{D_{f_i}}}{2} + 2\right)\left(\frac{\rho_2}{\rho_3} - 1\right)$$

The ratio $\Delta p/p_3$ can therefore be expressed as a function of M_3^2. A Maclaurin expansion of the function $\Delta p/p_3$ gives

$$\frac{\Delta p}{p_3} = \beta_1 M_3^2 + \beta_2 \left(M_3^2\right)^2 + \ldots \beta_n \left(M_3^2\right)^n + \ldots \qquad (11)$$

The coefficients β_1 and β_2 are obtained from equation (10) by calculating the first and second derivatives of $\Delta p/p_3$ with respect to M_3^2 and evaluating each derivative at $M_3^2 = 0$. The calculation of the first and second derivatives indicates that equation (11) is a rapidly convergent series and consequently the first term of equation (11) gives a very close approximation to one-dimensional flow theory. The first term gives results that differ from the results obtained by one-dimensional flow theory by not more than 5 percent when the exit Mach number is as high as 0.7. The value of the coefficient β_1 is

$$\beta_1 = \frac{\gamma}{2}\frac{1}{1 + T'}\left[1 + C_{D_{f_i}} + \left(\frac{C_{D_{f_i}}}{2} + 2\right)T'\right]$$

and the series given by equation (11) can therefore be closely approximated as

$$\frac{\Delta p}{q_3} = \frac{1}{1 + T'}\left[1 + C_{D_{f_i}} + \left(\frac{C_{D_{f_i}}}{2} + 2\right)T'\right] \qquad (12)$$

Equation (12) indicates that the coefficient $\Delta p/q_3$ is a function of only the heat dissipated and the drag coefficient. For the case of no heat transfer, $T' = 0$, equation (12) becomes simply

$$\left(\frac{\Delta p}{q_3}\right)_i = 1 + C_{D_{f_i}} \qquad (13)$$

The relation between the pressure-drop coefficients with and without heat transfer can be found, from equations (12) and (13), to be

$$\frac{\Delta p}{q_3} = \left(\frac{\Delta p}{q_3}\right)_i \frac{1 + T'/2}{1 + T'} - \frac{3}{2}\frac{T'}{1 + T'} \qquad (14)$$

It therefore appears possible, in addition to correcting for compressibility effects, to obtain the pressure-drop coefficient $\Delta p/q_3$ on a cold cylinder and then to calculate the coefficient with heat transfer from equation (14).

Characteristic Mach Number Method

A second empirical method of eliminating compressibility effects uses a compressibility correction factor to relate the pressure drops for compressible and incompressible flow as

$$\Delta p = \frac{\rho_s}{\rho_o} \frac{\Delta p_s}{\sqrt{1 - M_o^2}}$$

where M_o is a Mach number characteristic of the flow at some point along the fin-baffle passage (reference 2). A relation between this method and one-dimensional flow theory also exists and can be shown as follows: If the Maclaurin expansion is developed in terms of a Mach number M_x characteristic of the flow at some point x along the fin-baffle passage, the following series results:

$$\frac{\Delta p}{p_x} = \alpha_1 (M_x)^2 + \alpha_2 \left(M_x^2\right)^2 + \ldots \alpha_n \left(M_x^2\right)^n + \ldots \qquad (15)$$

Equation (15) may be divided by M_x^2 and the resulting series inverted and squared to give

$$\left(\frac{1}{\Delta p/q_x}\right)^2 = \frac{1}{\alpha_1^2} - 2\frac{\alpha_2}{\alpha_1^3} M_x^2$$

where powers of M_x greater than 2 are neglected.

The square root of the foregoing equation is then

$$\frac{1}{\Delta p/q_x} = \frac{1}{\alpha_1}\sqrt{1 - 2\frac{\alpha_2}{\alpha_1} M_x^2} \qquad (16)$$

For the same air flow at sea level the characteristic Mach number is very small and

$$\frac{1}{\Delta p_s/q_s} \approx \frac{1}{\alpha_1}$$

Consequently

$$\Delta p = \frac{\rho_s}{\rho_x} \frac{\Delta p_s}{\sqrt{1 - 2\left(\frac{\alpha_2}{\alpha_1}\right) M_x^2}}$$

The definition of the characteristic Mach number can be chosen to make $\alpha_2/\alpha_1 = 1/2$. Equation (17) then reduces to the form given in reference 2

$$\Delta p = \frac{\rho_s}{\rho_o} \frac{\Delta p_s}{\sqrt{1 - M_o^2}} \tag{18}$$

A method of trial and error must be used to determine from experimental data the characteristic Mach number for a particular cylinder-baffle arrangement in order that equation (18) be valid. Equation (18) may be applied analytically by using conditions at the baffle exit as those characteristic of the flow. Thus in equation (17)

$$\alpha_1 = \frac{\gamma}{2} \beta_1$$

and

$$\alpha_2 = \frac{\gamma}{2} \beta_2$$

In general,

$$\frac{\beta_2}{\beta_1} < \frac{1}{2}$$

and therefore

$$\frac{\alpha_2}{\alpha_1} < \frac{1}{2}$$

The application of equation (18) should then give higher predicted pressure-drop values than equation (17) when the baffle-exit density determines the characteristic state. Satisfactory results were obtained (reference 2) when the characteristic state was determined by the stagnation pressure upstream of the cylinder, the stagnation temperature downstream of the cylinder, and the mass flow of cooling air.

APPLICATION OF BAFFLE-EXIT DENSITY METHOD

Two methods of applying the one-dimensional flow theory are presented in references 1 and 3, but the use of the baffle-exit density method is impracticable because the static temperature at the baffle exit is difficult to measure. The stagnation temperature at the baffle exit can be measured and if, in the pressure-drop coefficient, the true baffle-exit density is replaced by the density determined by the static pressure and the stagnation temperature at the baffle exit, the value of the coefficient will closely approximate that obtained by means of one-dimensional flow theory. If this density is designated $\bar{\rho}_3$, the corresponding Mach number and velocity pressure $\bar{M}_3$ and $\bar{q}_3$ are given by

$$\bar{M}_3^2 = \frac{G^2}{\gamma p_3 \bar{\rho}_3}$$

and

$$\bar{q}_3 = \frac{G^2}{2\bar{\rho}_3}$$

From the previous analysis the new coefficients $\bar{\beta}_1$ and $\bar{\beta}_2$, in the series expansion given by equation (11), are

$$\bar{\beta}_1 = \beta_1$$

and

$$\bar{\beta}_2 = 0.4\beta_2$$

The use of either $\bar{q}_3$ or q_3 thus gives the same degree of approximation to one-dimensional flow theory.

A simple method of predicting the pressure drop based on the density $\bar{\rho}_3$ can now be used. In the case where the pressure loss at the baffle exit is small, the cylinder pressure drop is simply

$$\Delta p = p_{1_t} - p_3$$

or

$$\frac{p_{1_t} - p_3}{\Delta p} = 1 \qquad (19)$$

When a significant pressure change occurs at the baffle exit, the ratio given by equation (19) will differ from unity. If the assumption is made that the percentage of the over-all pressure drop which occurs at the baffle exit will not change with altitude, equation (19) may be expressed generally as

$$\frac{p_{l_t} - p_3}{\Delta p} = K \tag{20}$$

Then

$$p_3 = p_{l_t} - K\Delta p$$

The pressure-drop coefficient $\Delta p/\bar{q}_3$, or $2\bar{\rho}_3 \Delta p/G^2$, is a function of the Reynolds number. For a given fin-baffle arrangement, however, the characteristic length is fixed and consequently the Reynolds number varies only with the mass flow of cooling air G and the cooling-air viscosity μ; therefore, if the Reynolds number at sea level and at a given altitude are equal, the mass flow of cooling air at the altitude condition can be reduced to the equivalent mass flow of cooling air at sea level $G\mu_s/\mu_o$. The quantity μ_s is the standard sea-level viscosity and μ_o is the actual viscosity at altitude or at the condition under which pressure-drop computations are made. The pressure-drop coefficient $\Delta p/\bar{q}_3$ may thus be written as

$$\frac{2\bar{\rho}_3 \Delta p}{G^2} = f\left(G\frac{\mu_s}{\mu_o}\right) \tag{21}$$

The stagnation temperature at the baffle exit is assumed equal to the downstream stagnation temperature and is obtained from sea-level heat-transfer data. The heat dissipated per pound of cooling air is calculated by means of stagnation temperatures (reference 6) and is given by

$$H = c_p\left(T_{3_t} - T_{l_t}\right) \tag{22}$$

The value of H can also be expressed in a manner similar to that of reference 7 as

$$H = S\,G^m\left(T_h - T_{l_t}\right) \tag{23}$$

where S and m are constants determined from sea-level tests. The solution of equations (22) and (23) for T_{3_t} gives

$$T_{3_t} = \frac{SG^m}{c_p}\left(T_h - T_{l_t}\right) + T_{l_t} \tag{24}$$

which is the value of T_{3_t} at the baffle exit of the cylinder head. A similar expression will hold for the barrel.

The density $\bar{\rho}_3$ is expressed

$$\bar{\rho}_3 = \frac{p_3}{RT_{3_t}} = \frac{p_{1_t} - K\Delta p}{RT_{3_t}} \tag{25}$$

The substitution of this relation in equation (21) gives

$$\frac{2\bar{\rho}_3 \Delta p}{G^2} = \frac{2\left(p_{1_t} - K\Delta p\right)\Delta p}{G^2 RT_{3_t}} = f\left(\frac{G\mu_s}{\mu_o}\right) \tag{26}$$

which, when solved for Δp, becomes

$$\Delta p = \frac{1}{2K}\left\{p_{1_t} - \left[p_{1_t}^2 - 2KRT_{3_t} G^2 f\left(G\frac{\mu_s}{\mu_o}\right)\right]^{1/2}\right\} \tag{27}$$

The value of G is obtained from the basic cooling-correlation equation (reference 7) and the viscosity ratio is calculated from the average of the cylinder-head or cylinder-barrel temperatures and the cooling-air temperature. The coefficient $2\bar{\rho}_3 \Delta p/G^2$ is obtained from a sea-level calibration curve based on tests with heat transfer and the value of K is also determined from sea-level data, although in most cases K will probably be sufficiently close to unity that it may be neglected. The altitude and the pressure rise in front of the engine due to the velocity of the airplane determine the value of p_{1_t} and the pressure drop across the engine can then be evaluated from equation (27).

APPARATUS AND INSTRUMENTATION

Test equipment. - The accuracy of the various methods of estimating the effect of altitude on the relation between the pressure drop and the cooling-air weight flow was investigated on a rear-row cylinder from a typical 18-cylinder air-cooled engine equipped with standard flight baffles (fig. 1) and mounted on a converted multicylinder crankcase. Front-row baffles were installed upstream of the test cylinder to simulate flight air-flow conditions. The cylinder was enclosed within an airtight duct through which cooling air was supplied at temperature and pressure conditions ranging from sea level to 40,000 feet. Automatic controls in the air-supply system maintained the cooling-air conditions upstream of the cylinder within ±0.05 inch of mercury and within ±4° F of the desired values. The quantity of cooling air was measured by means of an adjustable orifice located upstream of the test section and the pressure drop across the orifice was indicated by an alcohol-filled micromanometer. The cooling-air weight measurements were accurate within ±1 percent.

A straight section of pipe extended approximately 10 diameters in front of the cylinder. The power developed by the engine was absorbed by a dynamometer and an inductor coupled as a unit.

Cylinder instrumentation. - The cooling-air pressures at the baffle inlet and outlet were measured with open-end tubes located as shown in figure 2. The tubes had a wall thickness of 0.006 inch and an outside diameter of 0.040 inch and were placed midway between the fin root and the fin tip. Static pressures, which were taken only at the baffle outlet, were measured by open-end tubes placed flush with the fin surfaces as shown in figure 2(c). The total-pressure and static-pressure tubes at the baffle outlet were located in adjacent fin spaces. The pressure drop across the cylinder was indicated by the pressure difference between two static piezometer rings located upstream and downstream of the cylinder. Each ring consisted of four interconnected taps; one tap was located in each of the four sides of the cooling-air duct.

The cooling-air temperature at the front of the cylinder was measured by two iron-constantan thermocouples located in the center of the cooling-air duct $2\frac{1}{2}$ feet in front of the cylinder. The temperature of the cooling air leaving the cylinder was measured by shielded iron-constantan thermocouples placed at four locations behind the cylinder head and at four locations behind the cylinder barrel. Cylinder temperatures were measured by iron-constantan thermocouples peened into the cylinder at 22 places on the head and 10 places on the barrel. The location of the cylinder thermocouples was similar to that shown in figure 7 of reference 8.

TESTS AND CALCULATIONS

The validity of the one-dimensional flow analyses may be established by showing that the coefficients $C_{D_{f_i}}$ and F are functions of only the Reynolds number and are independent of compressibility effects. If such a relation exists for $C_{D_{f_i}}$ and F, then from the analysis the pressure-drop coefficient $\Delta p/\bar{q}_3$ will be approximately independent of compressibility effects, but the extent to which the compressibility effects are eliminated must be experimentally demonstrated. An investigation must also be made to determine whether, for an actual cylinder, a characteristic Mach number can be found that is suitable for use in the correction factor $\rho_o\sqrt{1 - M_o^2}$. The effect of heat transfer on each of the foregoing methods of estimating pressure drop must also be determined.

Tests were conducted to obtain data permitting evaluation of the drag and cylinder pressure-drop coefficients over a wide range of air flows.

Tests without heat transfer. - Tests were first conducted without heat transfer. The flow of cooling air over the cylinder head and the cylinder barrel was separately determined by blocking each section and causing the air to flow over only the unblocked section. The air flow across the flange and the barrel was separated in order that a more accurate value of the mass velocity of the cooling air G might be determined for the barrel without the flange.

The entire cylinder was also blocked to determine the leakage around the outside of the baffles. In each case the cooling-air weight, the pressure and the temperature at the front of the cylinder, the pressure at the rear of the cylinder, and the pressures at the baffle inlet and at the baffle outlet of the unblocked section of the cylinder were measured. These tests were conducted at density altitudes corresponding to sea level, 15,000 feet, 30,000 feet, and 40,000 feet based on Army standard summer-air temperatures.

Tests with heat transfer. - Tests at these same altitudes were conducted at four engine powers. In addition to the measurements taken during the tests without heat transfer, the cooling-air temperature at the rear of the cylinder was recorded. Because the distribution of the cooling-air between the cylinder head and the cylinder barrel could not be determined, the total cooling-air flow over the entire cylinder was measured.

Calculations (data without heat transfer). - The evaluation of the drag coefficient $C_{D_{f_i}}$ requires that the state of the cooling air at the baffle inlet and outlet be known. For tests without heat transfer the values of $C_{D_{f_i}}$ were found from equation (5) which can be more conveniently written as

$$\frac{2\,\rho_2\,(p_2 - p_3)}{G_2} = \frac{C_{D_{f_i}}}{2}\left(\frac{\rho_2}{\rho_3} + 1\right) + 2\left(\frac{\rho_2}{\rho_3} - 1\right) \qquad (28)$$

The values of G for the cylinder head and the cylinder barrel were calculated from the measured cooling-air weight and the free-flow area of the fin-baffle passage. The density at the front of the cylinder was determined from the measured pressure and temperature at that point and the pressure p_2 was then obtained from equation (1b). The temperature at the baffle inlet followed from

the isentropic temperature-pressure relation and the density ρ_2 was evaluated from the values of p_2 and T_2. Experimental values were used for p_3. The density ratio ρ_2/ρ_3 and $C_{D_{f_i}}$ were then evaluated by means of equation (28) and the curves of figure 5 in reference 1.

In reference 3, the calculation of the pressure drop across the cylinder was simplified by evaluating the pressure drop exactly by means of equations (1b), (3), and (4) and then plotting the ratio $\Delta p/p_{1_t}$ as a function of its value at low Mach numbers

$$\frac{G^2}{2p_{1_t}\rho_{1_t}}\left(1 + \frac{\Delta T}{2T_{1_t}}\right)\left(1 + F + \frac{\Delta T}{T_{1_t}}\right)$$

Curves of this type, using $\Delta T/T_{1_t}$ and F as parameters, are given in figure 10 of reference 3. The coefficient F was determined from these curves for known values of Δp, p_{1_t}, ρ_{1_t}, and T_{1_t}. The cooling-air temperature rise ΔT was zero for the tests without heat transfer.

The pressure-drop coefficient $\Delta p/\bar{q}_3$, or $2\bar{\rho}_3 \Delta p/G^2$, was evaluated from measured values of G, Δp, p_3, and T_{1_t}; the temperature T_{1_t} was used instead of T_{3_t} for the data without heat transfer.

The characteristic Mach number factor $\rho_o\sqrt{1 - M_o^2}$ was evaluated from measured values of G, p_{1_t}, T_{1_t}, and the curves of figure 2 in reference 2.

Calculations (data with heat transfer). - The coefficients $C_{D_{f_i}}$ and F could not be directly determined for the data with heat transfer because the air flow over the head and the barrel could not be individually measured. The pressure-drop coefficient $\Delta p/\bar{q}_3$, however, was evaluated for the cylinder as a whole; the stagnation temperature at the rear of the cylinder was used for T_{3_t}.

In order to examine still further the effect of heat transfer, the pressure drop required with heat transfer at altitude was calculated by each method except the one utilizing the characteristic Mach number. A method of successive approximations was used to determine the distribution of cooling air across the head and the barrel. The distribution was first assumed to be the same as that found in the tests without heat transfer and corresponding values of pressure

drop across the head and the barrel were calculated by equations (5), (7), and (9). The experimental pressure drops across the head and the barrel were the same and therefore any difference in the calculated values was assumed to result from a change in the cooling-air distribution obtained from tests without heat transfer. A correction to the air distribution was made by adjusting the assumed barrel air flow until the pressure drop across the barrel agreed with that for the head.

Pressure-drop predictions by means of the method based on the static pressure and the stagnation temperature at the baffle exit were made from equation (27).

RESULTS AND DISCUSSION

Evaluation of Data

The usual manner of calibrating the air flow over the head and the barrel of a cylinder consists in plotting the cooling-air weight flow against the product of the cooling-air pressure drop and the ratio of the mean entrance and exit density to the standard sea-level air density. Curves of this type were determined (fig. 3) for several altitudes with data obtained without heat transfer. The wide systematic variation indicates that a sea-level calibration of this type cannot be used accurately at any altitude beyond the value of pressure drop at which the deviation from the sea-level curve is significant. The divergence of the altitude curves will increase with the addition of heat. Similar compressibility effects were observed in the tests of reference 2. The methods that account for these compressibility effects may be evaluated by observing whether the data for all altitudes fall on one curve or, more precisely, if the drag or pressure-drop coefficients used are functions of only the Reynolds number. An uncorrected compressibility effect exists if, in the plot of drag or cylinder pressure-drop coefficient against Reynolds number (proportional to $G\mu_s/\mu_o$), the altitude data at high air flows indicate a rising curve. The greater the deviation of this rising curve from the sea-level curve the greater is the inaccuracy in the method of correction.

One-dimensional flow processes (without heat transfer). - The relation between $C_{D_{f_i}}$ and the corrected mass flow of cooling air (proportional to the characteristic Reynolds number) shows no definite trend with altitude (fig. 4) and is therefore considered independent of compressibility effects. The curves on this and subsequent figures are drawn through the sea-level data. The dispersion of the data at high values of air flow across the cylinder head is

explained by the unsymmetrical fin passages on the head. The friction-drag coefficient $C_{D_{f_i}}$, based on the mean of the dynamic pressures at the baffle ends, can be evaluated more accurately when the exit conditions are uniform, as on the cylinder barrel, than when they are exceedingly nonuniform due to unsymmetrical fin passages, as on the cylinder head.

The data points for the coefficient of pressure change across the baffle exit $C_3 - a_3$ scatter somewhat (fig. 5) for both the cylinder head and the cylinder barrel but the values are small compared with the baffle pressure-drop coefficients and may be neglected for the cylinder head. The relative magnitude of the pressure loss across the fin-baffle passage of the barrel and across the entire cylinder may be seen by plotting the ratio $p_{1_t} - p_3/\Delta p$ against $\Delta p/p_{1_t}$ as was done in figure 6. The pressure loss across the barrel baffle exit is about 10 percent of the entire cylinder pressure loss and therefore cannot be neglected in accurate calculations involving this particular cylinder barrel. Because the exit loss is a small part of the entire loss, moderate inaccuracies in the exit coefficient will have only a slight effect on the over-all pressure-loss coefficient. The sum of the pressure loss coefficients for the entrance process, the baffle flow process, and the exit process gives the over-all pressure-loss coefficient (reference 2) as

$$\frac{2\rho\Delta p}{G^2} = 1 + C_{D_{f_i}} + (C_3 - a_3) \tag{29}$$

where the exit coefficient given by equation (9) is used in place of the coefficient given by equation (8). The variation of the over-all pressure-loss coefficient with the corrected mass flow of cooling-air is shown in figure 7 for the cylinder head and the cylinder barrel. The correlation of the pressure-loss coefficients is satisfactory for all altitudes although a slight uncorrected compressibility effect for the cylinder head appears at 30,000 feet. This slight discrepancy may be neglected inasmuch as the effect does not appear at an altitude of 40,000 feet.

In the application of the one-dimensional flow analysis assuming uniform heat addition (reference 3), the value of the pressure-drop coefficient F is derived from the over-all pressure drop instead of the pressure drop across the baffle passage; consequently, when there is no heat transfer an equality exists between the over-all pressure-loss coefficient

$$\frac{2\rho\Delta p}{G^2} = 1 + F$$

and the over-all pressure-loss coefficient of equation (29). This observation is substantiated by comparing the relation between the coefficient $1 + F$ and the corrected mass flow of cooling air (fig. 8) with the similar relation for the coefficient $1 + C_{D_{f_i}} + (C_3 - a_3)$ (fig. 7).

Density-correction method (without heat transfer). - The pressure-loss coefficient based on the density determined by the static pressure and the stagnation temperature at the baffle exit is plotted against the corrected mass flow of cooling air in figure 9. The similarity between the relations shown in figures 7, 8, and 9 substantiates the relation given by equation (13), which showed that without heat transfer the pressure-loss coefficient $2 \bar{\rho}_3 \Delta p/G^2$ is very nearly $1 + C_{D_{f_i}}$. Therefore, when the baffle-exit coefficient is small, the density correction based on the static pressure and the stagnation temperature at the baffle exit provides a very close approximation to either of the one-dimensional flow methods.

The pressure-drop coefficient based on the downstream density was evaluated and is plotted in figure 10 to demonstrate the effect of the baffle-exit coefficient on correlating altitude-pressure-loss data. Because the pressure change across the baffle exit of the cylinder head is negligible, the results for the head are nearly identical with the density correction of figure 9. A measurable change of state takes place at the baffle exit of the cylinder barrel and the use of the downstream density overcorrects for the compressibility effect. The additional loss at the exit, however, can be accounted for by the use of the factor K in equation (27).

Characteristic Mach number (without heat transfer). - The incompressible-flow pressure-drop coefficient $2 \rho_o \sqrt{1 - M_o^2} \Delta p/G^2$ was evaluated by means of the upstream stagnation pressure and the downstream stagnation temperature and is plotted in figure 11 against the corrected mass flow of cooling air. The lack of correlation of the altitude data clearly shows that the effect of compressibility has not been eliminated.

A method of trial and error is required to determine the characteristic state that insures satisfactory application of the Mach number correction factor. The state determined by the upstream stagnation pressure and the downstream stagnation temperature, which gave good results in the tests of reference 2, does not appear to be generally applicable to all types of fin-baffle arrangement. Evaluation of the present data using various characteristic states gave

results that varied from those shown in figure 11 to a complete inversion of the same figure in which the compressibility effects were overcompensated. It must be concluded therefore that this type of correlation is not generally practical because of the difficulty in determining the characteristic state.

Application of methods to flow with heat transfer. - Because separate measurement of the cooling-air flow over the head and the barrel was impossible for the tests with heat transfer, the coefficients $C_{D_{f_i}}$ and F could not be evaluated. The combined flow over the head and the barrel was, however, obtained and used to show the effect of heat transfer on the pressure-drop coefficient based on the density determined by the average static pressure and the stagnation temperature at the baffle exit. The data were also evaluated by means of the downstream density. The average pressure-drop coefficients for the cylinder head and barrel combined are plotted in figure 12 as a function of the corrected average mass velocity of cooling air and are compared with the results without heat transfer. Except for the small compressibility effect for high air flows at 30,000 and 40,000 feet, which is evidenced by the slight upward trend of the data, figure 12(a) indicates that the pressure-drop coefficient based on the static pressure and the stagnation temperature at the baffle exit is independent of both altitude and wide variations in heat transfer. The pressure-drop coefficient based on the downstream density (fig. 12(b)) also appears to be unaffected by wide variations in heat transfer but, because of the pressure loss at the baffle exit of the barrel, the data for 30,000 and 40,000 feet fall below that at 15,000 feet and sea level at high air flows. The maximum spread of the data at 40,000 feet is $11\frac{1}{2}$ percent.

The average cylinder pressure-drop coefficient based on the average static pressure and the stagnation temperature at the baffle exit of the cylinder was evaluated for the data without heat transfer (fig. 12(c)) and the mean relations with and without heat transfer are compared in figure 12(d). A comparison of figures 12(a) and (c) shows an increased compressibility effect at 40,000 feet resulting from the addition of heat. The primary effect of heat transfer, however, was to raise the level of the pressure-drop coefficient; the difference between the coefficients with and without heat transfer became greater at low mass flows. The difference is much larger than predicted by equation (14). It appears that the increase in the pressure-drop coefficient occurs abruptly and that additional heating effects do not occur beyond the point of transition. The transition apparently results at engine conditions below normal operation and therefore is of no significance in practice.

Comparative Accuracy of Correction Methods

The effectiveness of each method of estimating the cooling-air pressure drop without heat transfer was evaluated by determining from figures 7 to 10 the percentage deviation of the altitude data from the sea-level calibration. Only the cylinder head was considered because it is usually the critical part. Points were taken at values of $\Delta p/p_{1_t}$ = 0.2, 0.3, 0.4, and 0.5. The method based on the characteristic Mach number correction $\sqrt{1 - M_o^2}$ was not evaluated because of the obvious lack of correlation shown by figure 11. The results are presented in the following table:

PERCENTAGE DEVIATION FROM SEA-LEVEL CALIBRATION

[+ above sea-level curve; - below sea-level curve]

Altitude (ft)	One-dimensional flow method based on F	One-dimensional flow method based on $C_{D_{f_i}}$	Density method based on static pressure and stagnation temperature at baffle exit	Density method based on downstream density
$\Delta p/p_{1_t}$ = 0.2				
15,000	+6.0	+6.6	+5.4	+5.3
30,000	+2.9	+2.8	0	0
40,000	+2.2	-4.3	-7.0	-4.4
$\Delta p/p_{1_t}$ = 0.3				
30,000	+6.3	+6.9	+6.3	+8.1
40,000	+2.8	0	-1.7	-1.1
$\Delta p/p_{1_t}$ = 0.4				
30,000	----------	+8.7	+9.3	+11.0
40,000	----------	0	0	-4.4
$\Delta p/p_{1_t}$ = 0.5				
30,000	----------	+9.9	+11.1	+12.7
40,000	----------	0	0	-5.0

At 30,000 feet all methods show a systematic increase in the deviation from the sea-level curve as the value of $\Delta p/p_{1_t}$ increases. At 40,000 feet, the density correction methods and the one-dimensional flow methods are equally accurate for all values of $\Delta p/p_{1_t}$ considered. The results for the method assuming uniform heat distribution were extended only to $\Delta p/p_{1_t}$ = 0.3, which was approximately the

maximum value used in the curves of reference 3. It appears, however, that this method will be applicable over the same range as the other methods. Estimates of pressure drop can therefore be made with the same accuracy by either the density correction or the one-dimensional flow methods.

A further comparison of the methods of estimating cooling-air pressure drop was made for tests with heat transfer by comparing the experimental pressure-drop data with pressure-drop values for similar cooling-air and engine conditions calculated with calibration curves obtained without heat transfer. For each method of predicting pressure drop the calculations were made at altitudes of 15,000 and 40,000 feet and at a cylinder brake horsepower of 56 to determine the pressure drops corresponding to given weights of cooling air flowing over the cylinder. The mass flow of cooling air was corrected for variation in viscosity caused by the addition of heat. The magnitude of the temperature rise across the cylinder at the power used in the calculations is shown in figure 13. Calculations were also made from the calibration curve of figure 3, which is based on the average cooling-air density across the engine. For this method an equation of the form

$$W = C\ (\sigma \Delta p)^{n} \tag{30}$$

was used. The values of C and n were determined from the sea-level curve of figure 3; consequently, equation (30) can be written

$$W_{h+b} = 0.406\ (\sigma_{av}\ \Delta p)^{0.517} \tag{31}$$

where W_{h+b} is the combined air flow over the head and the barrel.

The comparison of experimental and calculated results (fig. 14) shows that the experimental pressure-drop values are 10 to 15 percent higher than those calculated by any of the methods. The calculations were made with the curves of pressure-drop coefficients obtained from the tests without heat transfer. The results are the same as those indicated in figure 12(d). More accurate estimates of pressure drop can be made if the pressure-drop coefficients are obtained from curves based on tests with heat transfer. This observation was verified by calculating the pressure drops from the heat-transfer curve of figure 12(d). A comparison of the calculated pressure drops with the experimental results (fig. 15) shows that the agreement is good. Similar results are to be expected if $C_{D_{f_i}}$ and F are obtained from heat-transfer data. Accurate pressure-drop predictions can therefore be made by either of the one-dimensional flow methods or by the density correction method given in equation (27) if the pressure-drop coefficients are determined from sea-level tests with heat transfer.

Figure 15 further substantiates the accuracy of the density method of predicting pressure loss across an air-cooled cylinder at altitude. This method has the advantage of simplicity over the methods derived from one-dimensional flow theory.

SUMMARY OF RESULTS

A comparison of methods of predicting the compressible-flow pressure loss across a baffled, air-cooled cylinder and the evaluation of these methods by test data gave the following results:

1. The methods based on the density determined by the static pressure and the stagnation temperature at the baffle exit and the characteristic Mach number were shown by analysis to be close approximations to the methods derived by one-dimensional flow theory.

2. The experimental results obtained without heat transfer showed that the density method based on the static pressure and the stagnation temperature at the baffle exit and the methods derived by one-dimensional flow theory sufficiently eliminated the compressibility effects for the flow across both the head and the barrel of the cylinder tested. The use of the characteristic Mach number was found impractical because of the difficulty encountered in determining the characteristic state.

3. The pressure change across the baffle exit was negligible for the cylinder head but amounted to approximately 10 percent of the total pressure loss for the cylinder barrel.

4. The use of the density at the rear of the cylinder for the cylinder tested was satisfactory for the cylinder head but was slightly in error for the cylinder barrel.

5. The tests with heat transfer showed that the cylinder pressure-drop coefficient increased as a result of the addition of heat. The difference between the pressure-drop coefficients determined with and without heat transfer became greater as the mass flow of cooling air decreased. The difference was much greater than that predicted from one-dimensional flow theory.

6. Because of the unaccountable effect of heating, the use of the pressure-drop coefficients found from tests without heat transfer to predict pressure-drop requirements over a wide range of air flow at 15,000 and 40,000 feet for a given engine power resulted in an underestimation of the pressure drop by 10 to 15 percent. Predictions differing less than 10 percent from the experimental results were made by using the pressure-drop coefficients obtained from tests with heat transfer.

CONCLUSIONS

1. In order to make accurate compressible-flow pressure-drop predictions with the methods given in this report, the cylinder pressure-drop coefficient should be evaluated from tests with heat transfer.

2. The cylinder pressure-drop coefficient based on the static pressure and the stagnation temperature at the baffle exit can be used to make compressible-flow pressure-drop predictions with the same accuracy as the methods derived by one-dimensional flow theory.

Aircraft Engine Research Laboratory,
National Advisory Committee for Aeronautics,
Cleveland, Ohio, October 9, 1945.

REFERENCES

1. Becker, John V., and Baals, Donald D.: The Aerodynamic Effects of Heat and Compressibility in the Internal Flow Systems of Aircraft. NACA ACR, Sept. 1942.

2. Goldstein, Arthur W., and Ellerbrock, Herman H., Jr.: Compressibility and Heating Effects on Pressure Loss and Cooling of a Baffled Cylinder Barrel. NACA ARR No. E4G20, 1944.

3. Williams, David T.: High-Altitude Cooling. II - Air-Cooled Engines. NACA ARR No. L4I11a, 1944.

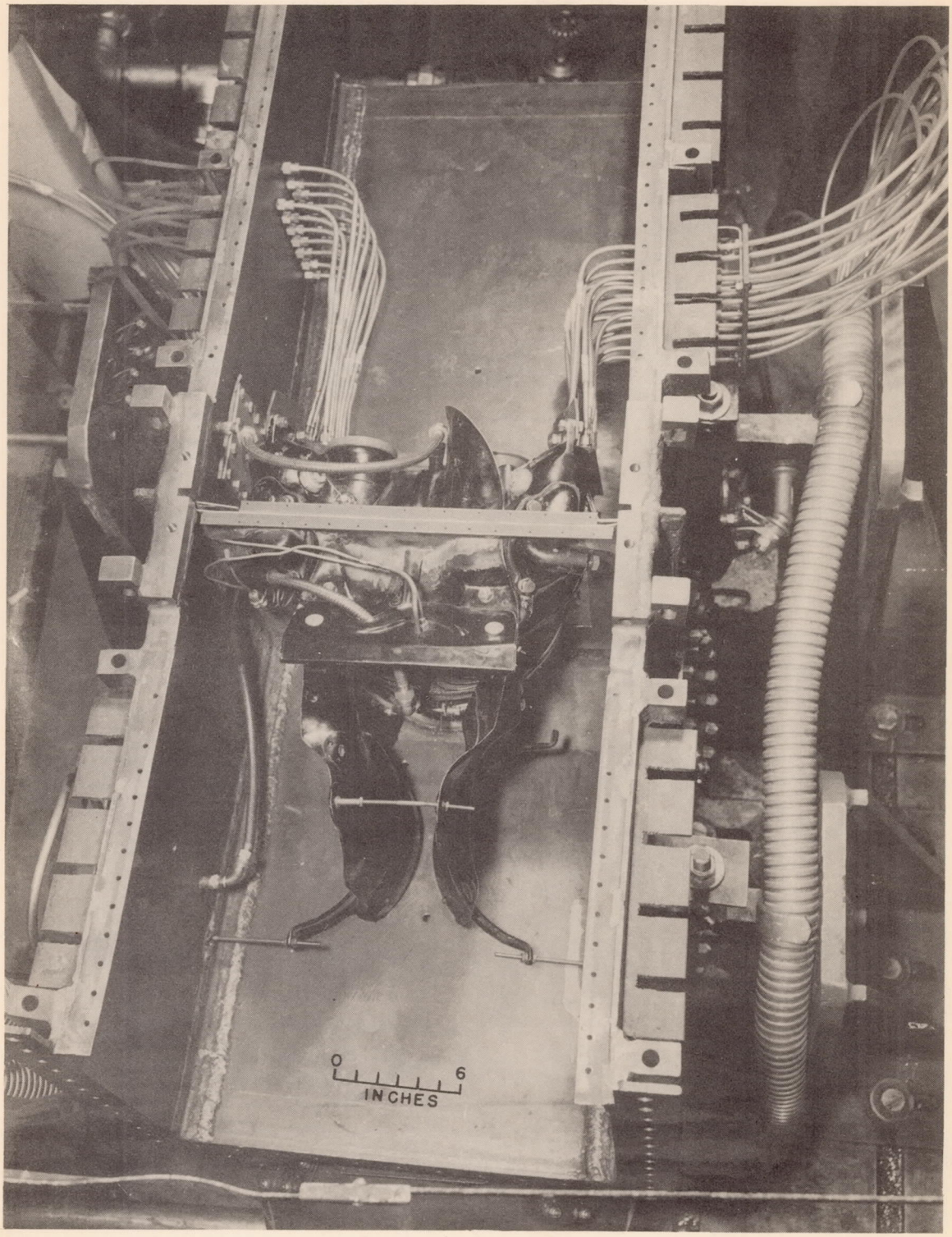
4. Erdman, Frank H., and Richards, W. M. S.: Report on Recommended Basic Revisions to Cooling Correlation Methods. W.A.C. Ser. No. 831, Wright Aero. Corp., July 1, 1943.

5. Pindzola, Michael: Cylinder Baffle Pressure Drop vs. Flow Characteristics of an Air-Cooled Engine Cylinder at Various Altitudes. PWA-505, Pratt & Whitney Aircraft, June 23, 1944.

6. Wood, George P.: Use of Stagnation Temperature in Calculating Rate of Heat Transfer in Aircraft Heat Exchangers. NACA RB No. 3J30, 1943.

7. Pinkel, Benjamin: Heat-Transfer Processes in Air-Cooled Engine Cylinders. NACA Rep. No. 612, 1938.

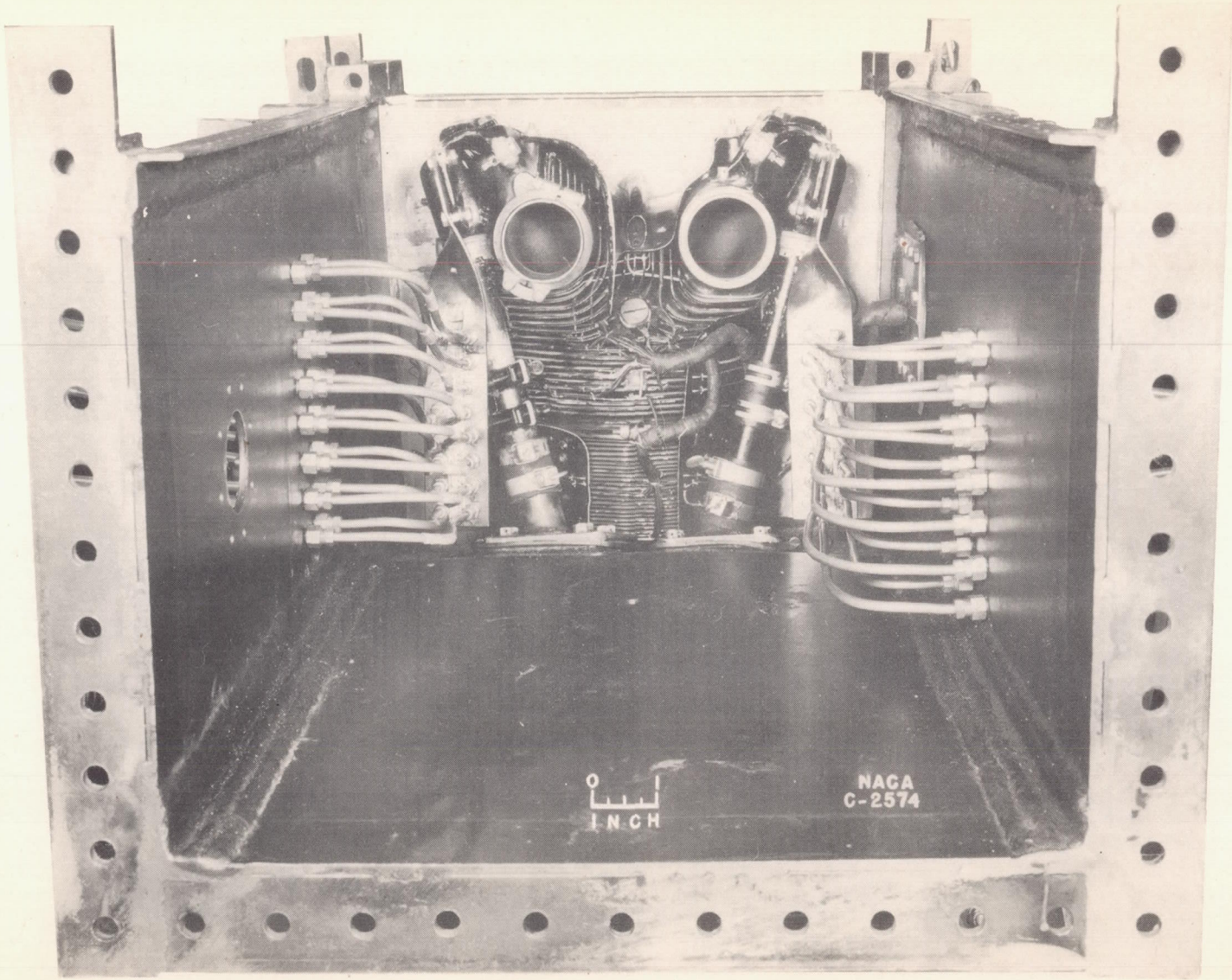
8. Schey, Oscar W., Rollin, Vern G., and Buckner, Howard A., Jr.: Comparative Cooling of Cylinders of Nonuniform Fin Width with Tight-Fitting Baffles and with Baffles That Provide Constant Flow-Path Areas. NACA ARR No. E4D21, 1944.



(a) Top view.

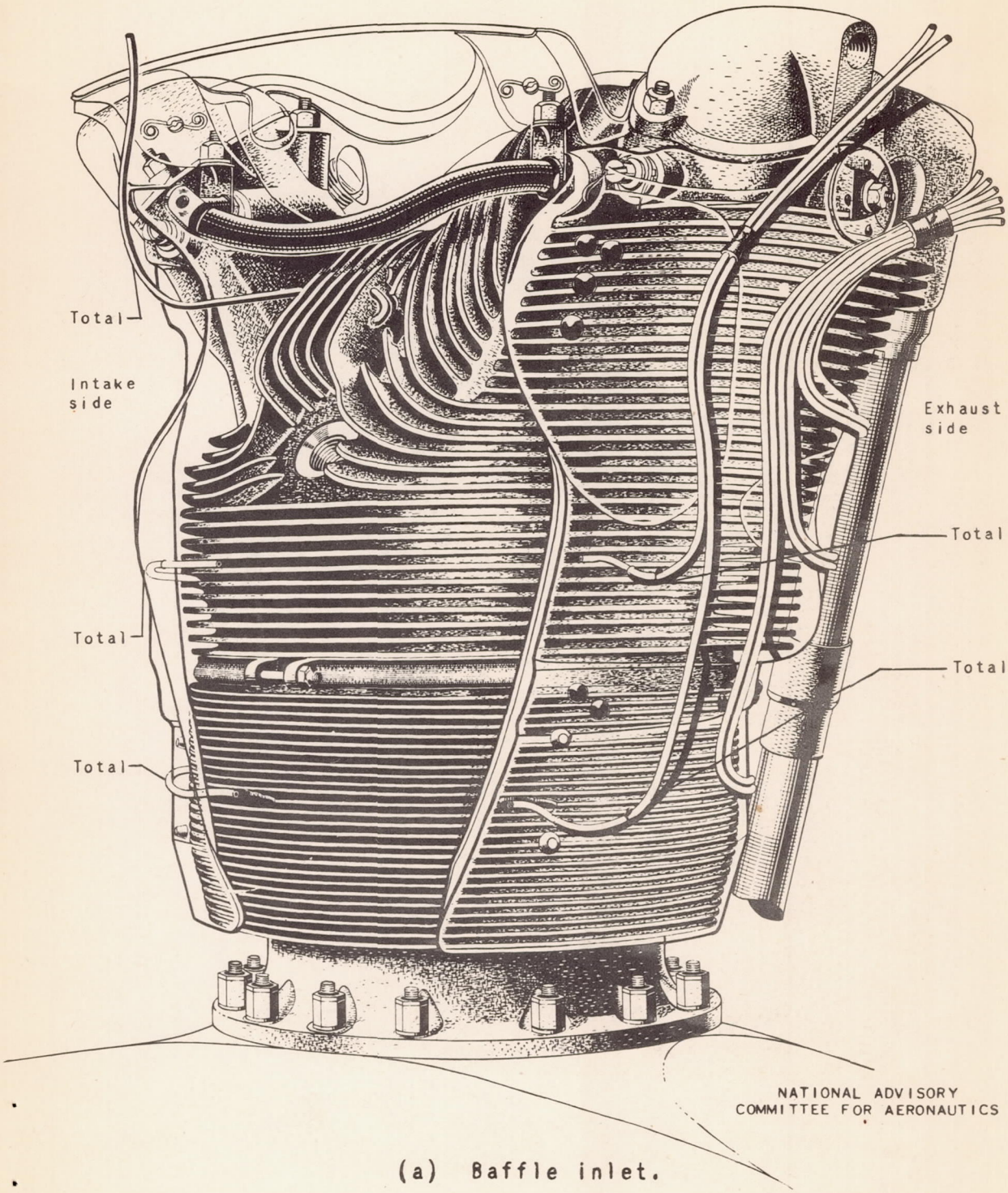
NACA
C-2577

Figure 1. - Test cylinder and flight baffles installed in test jacket.



(b) Rear view.

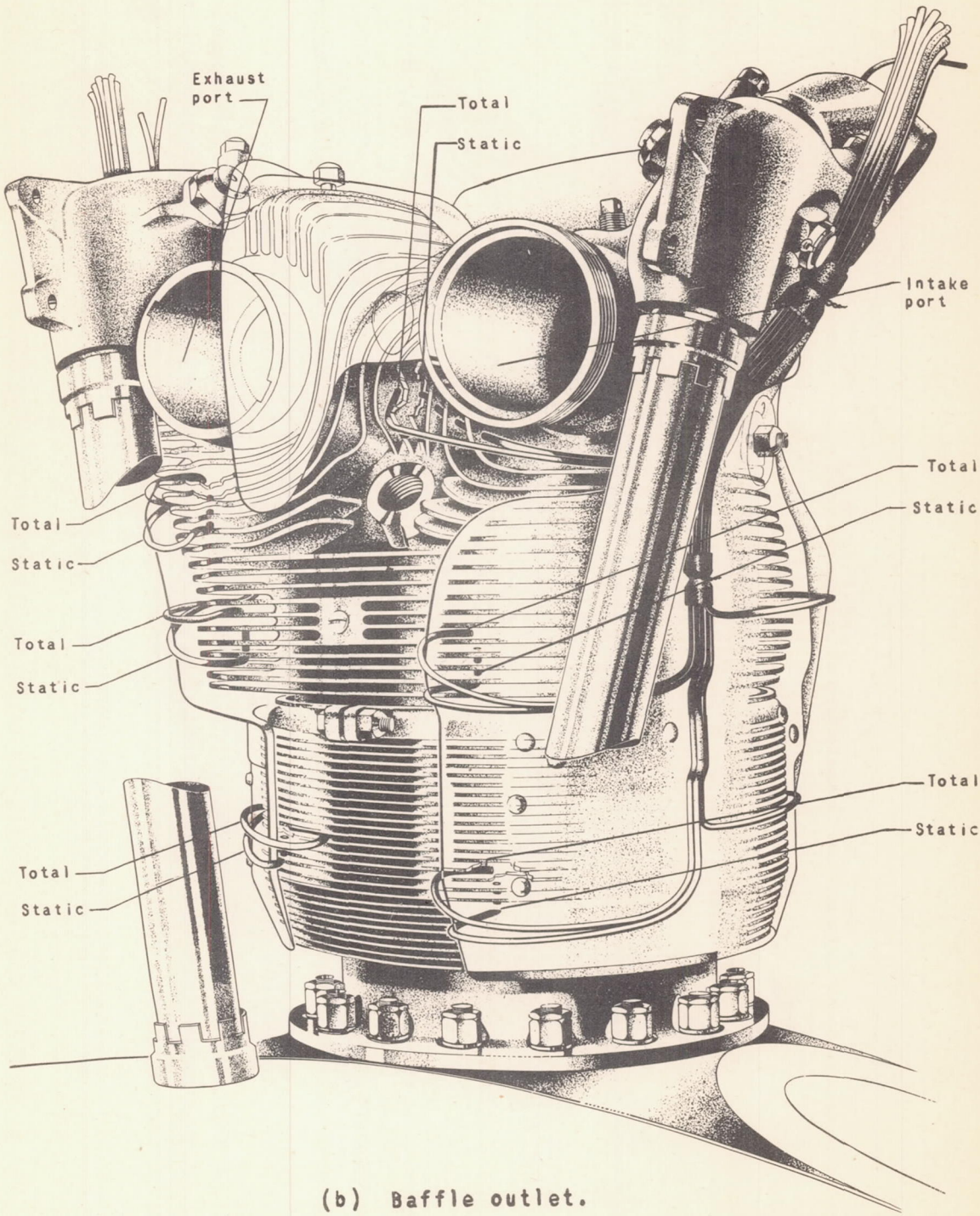
Figure 1. - Concluded.



(a) Baffle inlet.

Figure 2. - Pressure-tube locations on the test cylinder with flight baffles.

150+226

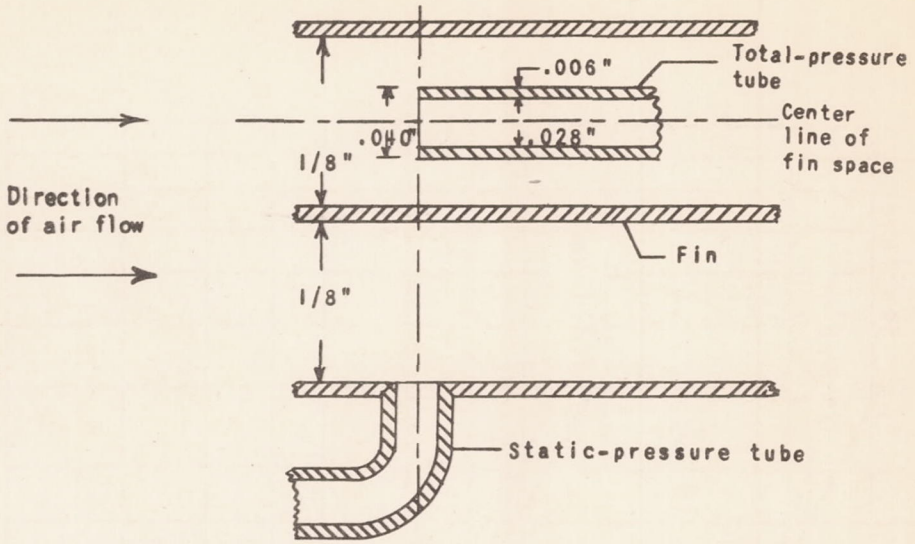


(b) Baffle outlet.

Figure 2. - Continued.

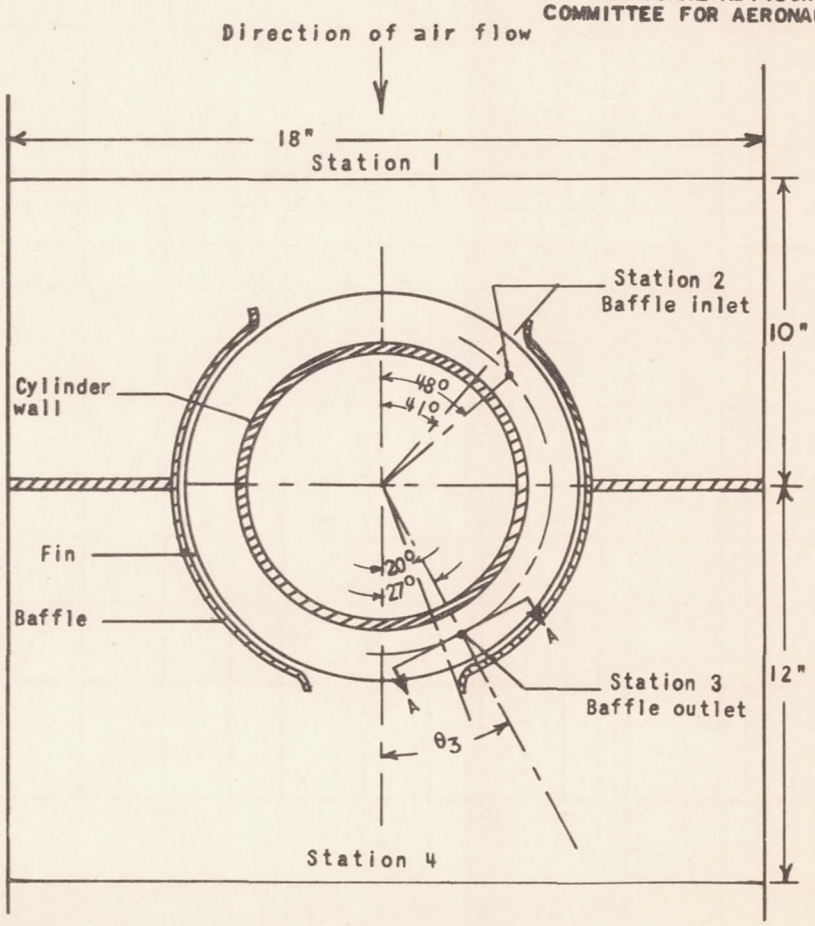
NATIONAL ADVISORY COMMITTEE FOR AERONAUTICS

150+232



Section A-A showing fin space and pressure-tube proportions

NATIONAL ADVISORY COMMITTEE FOR AERONAUTICS



(c) Location of pressure-measuring stations.

Figure 2. - Concluded.

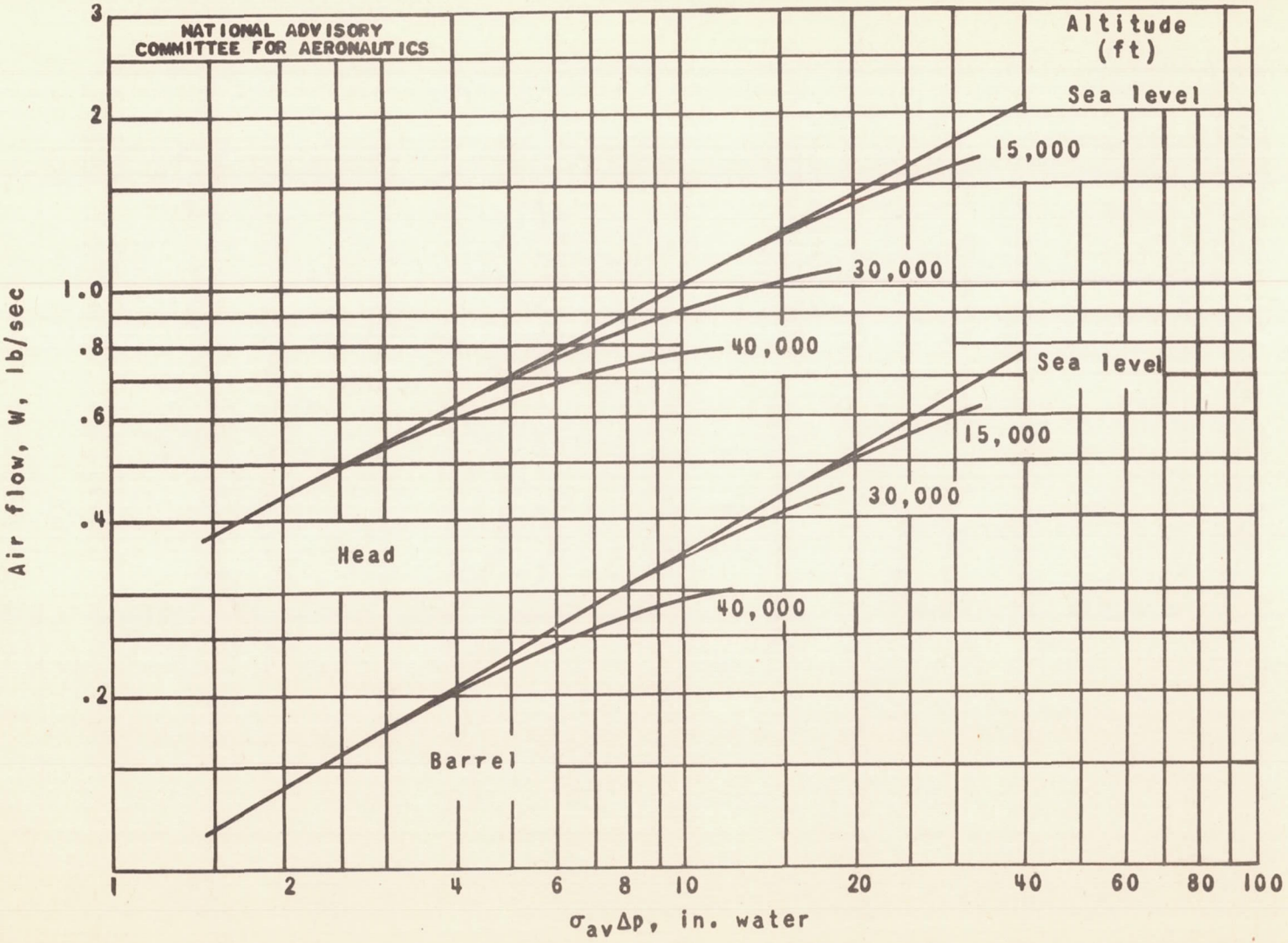


Figure 3. - Calibration curve of cooling-air weight flow; data without heat transfer.

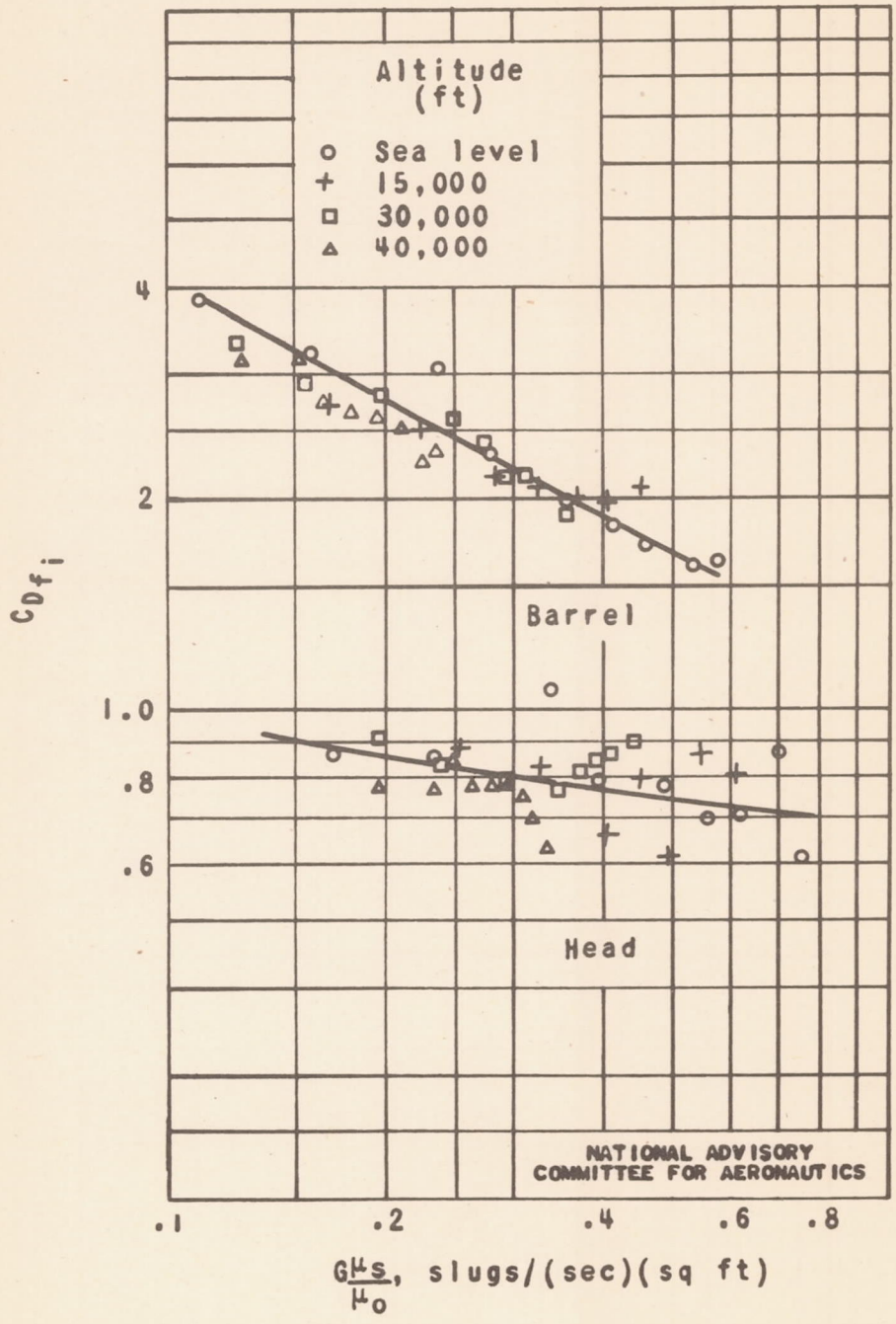


Figure 4. - Variation of friction-drag coefficient $C_{D_{f_i}}$ with corrected mass flow of cooling air; data without heat transfer.

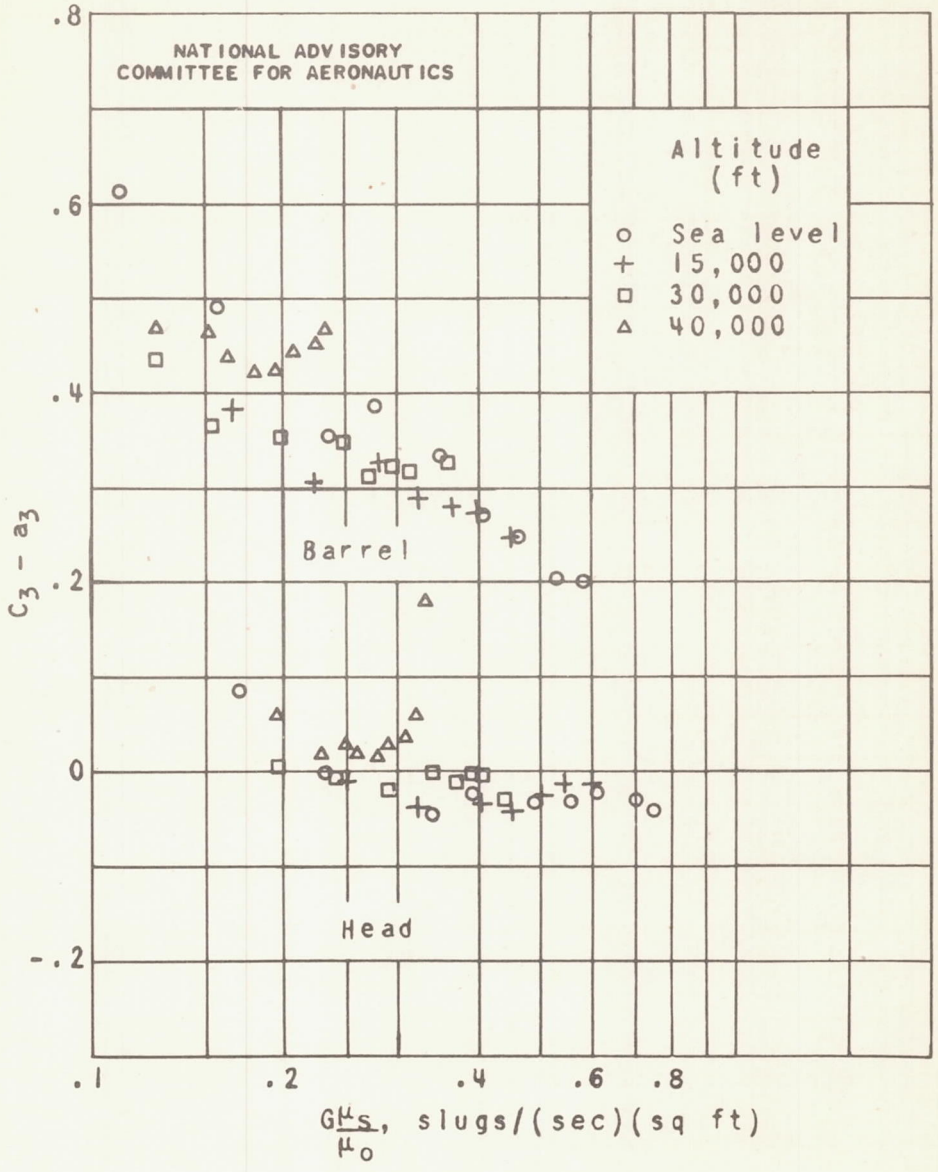


Figure 5. - Variation of baffle-exit pressure-loss coefficient with corrected mass flow of cooling air; data without heat transfer.

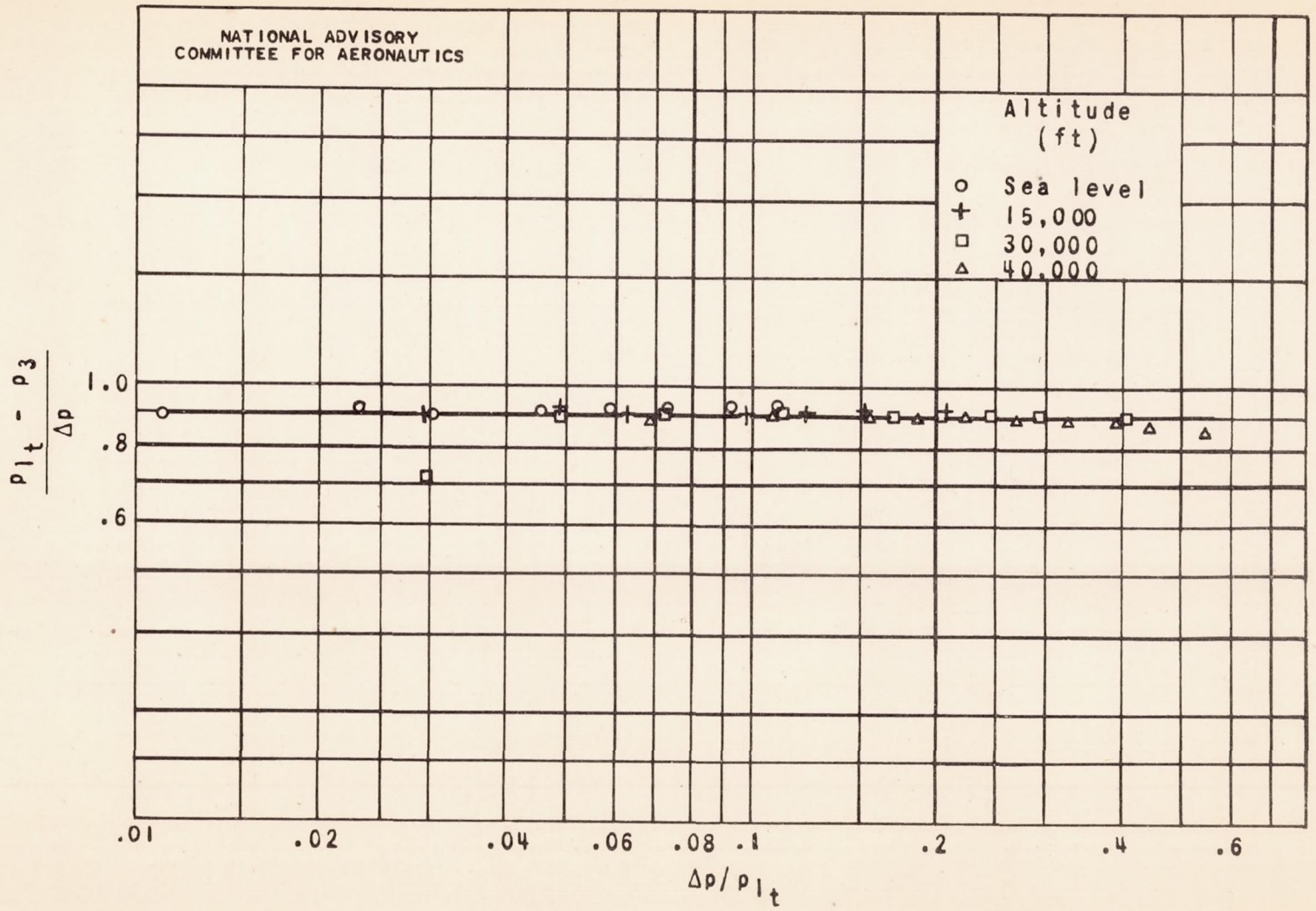


Figure 6. - Relation between pressure loss across fin-baffle passage of cylinder barrel and pressure loss across entire cylinder; data without heat transfer.

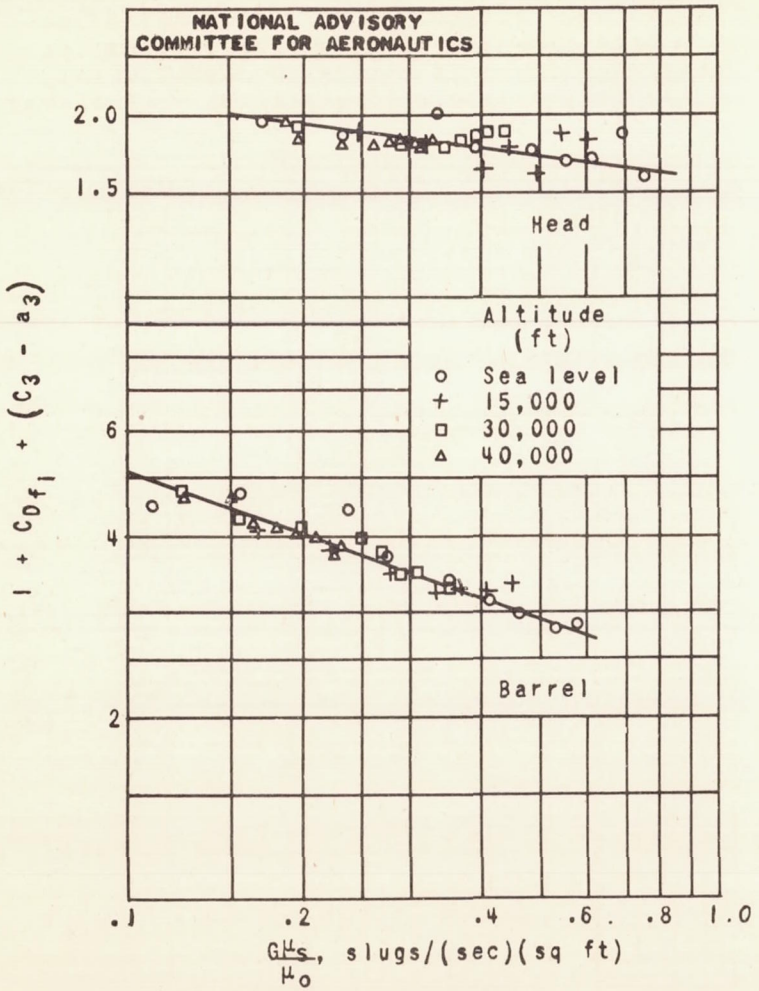


Figure 7. - Variation of over-all pressure-loss coefficient with corrected mass flow of cooling air for one-dimensional flow method assuming uniform dynamic pressure rise along fin-baffle passage; data without heat transfer.

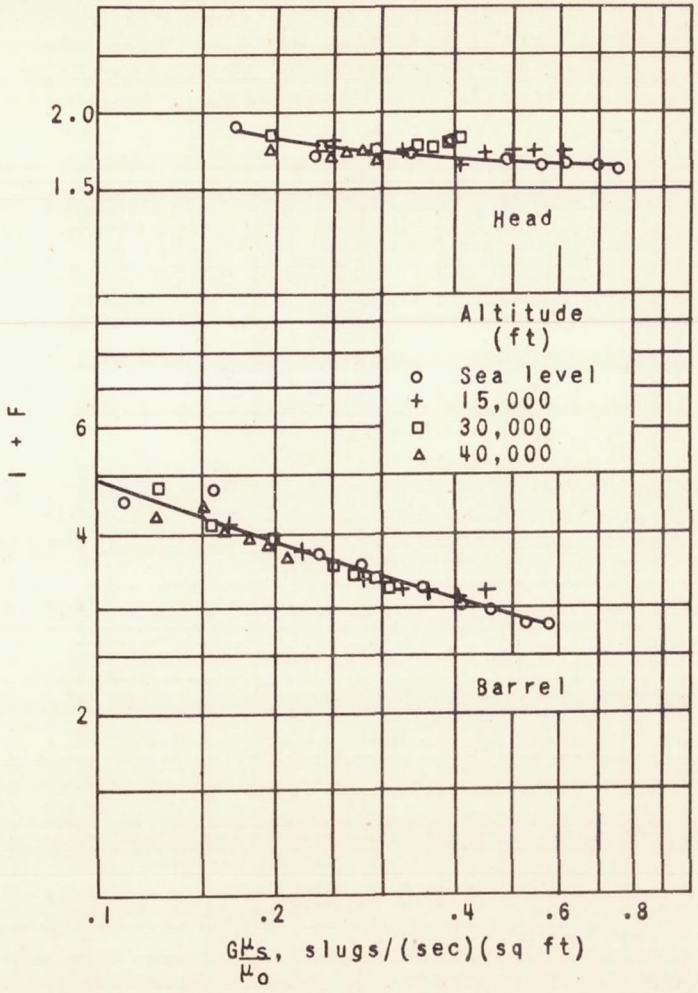


Figure 8. - Variation of over-all pressure-loss coefficient with corrected mass flow of cooling air for one-dimensional flow method assuming uniform temperature rise along fin-baffle passage; data without heat transfer.

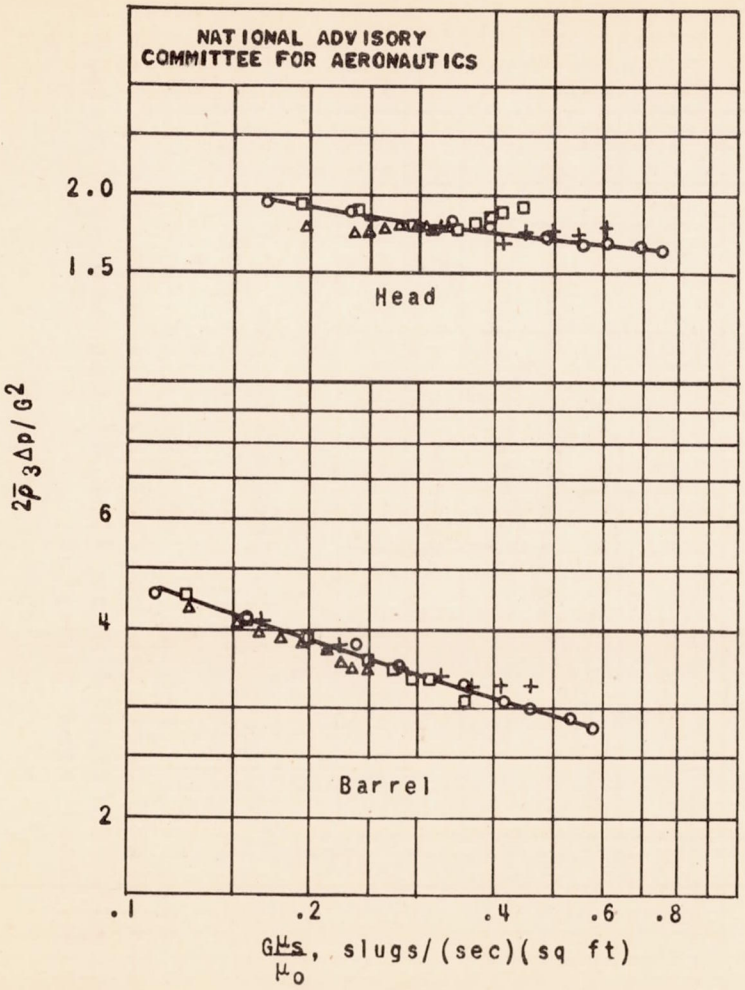


Figure 9. - Variation of pressure-loss coefficient based on static pressure and stagnation temperature at baffle exit with corrected mass flow of cooling air; data without heat transfer.

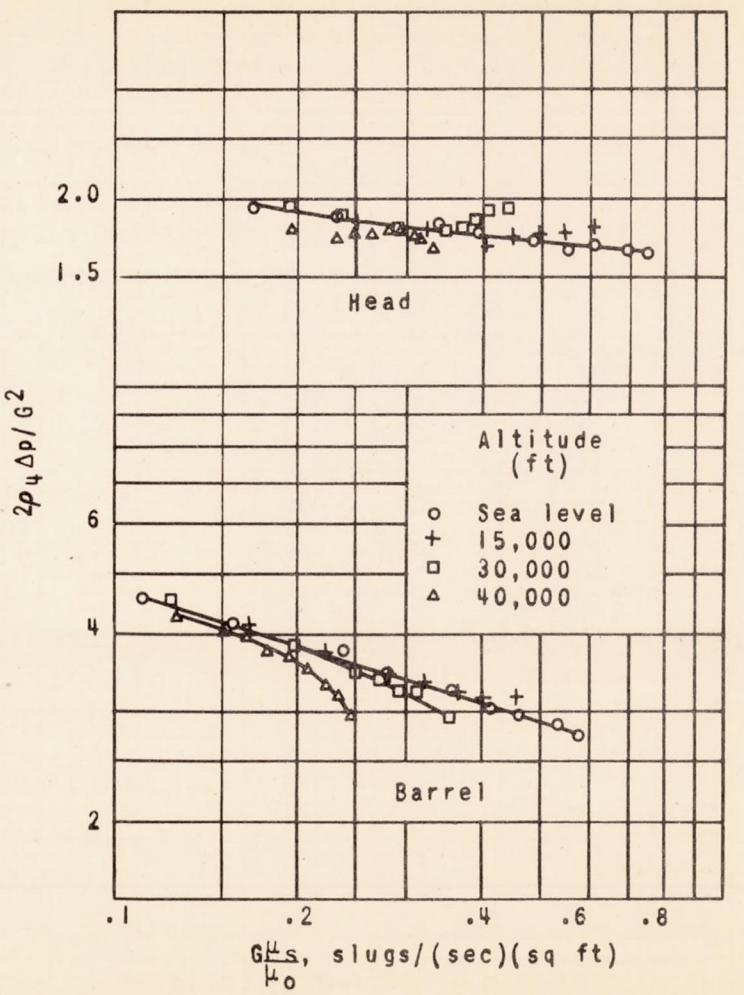


Figure 10. - Variation of pressure-loss coefficient based on downstream density with corrected mass flow of cooling air; data without heat transfer.

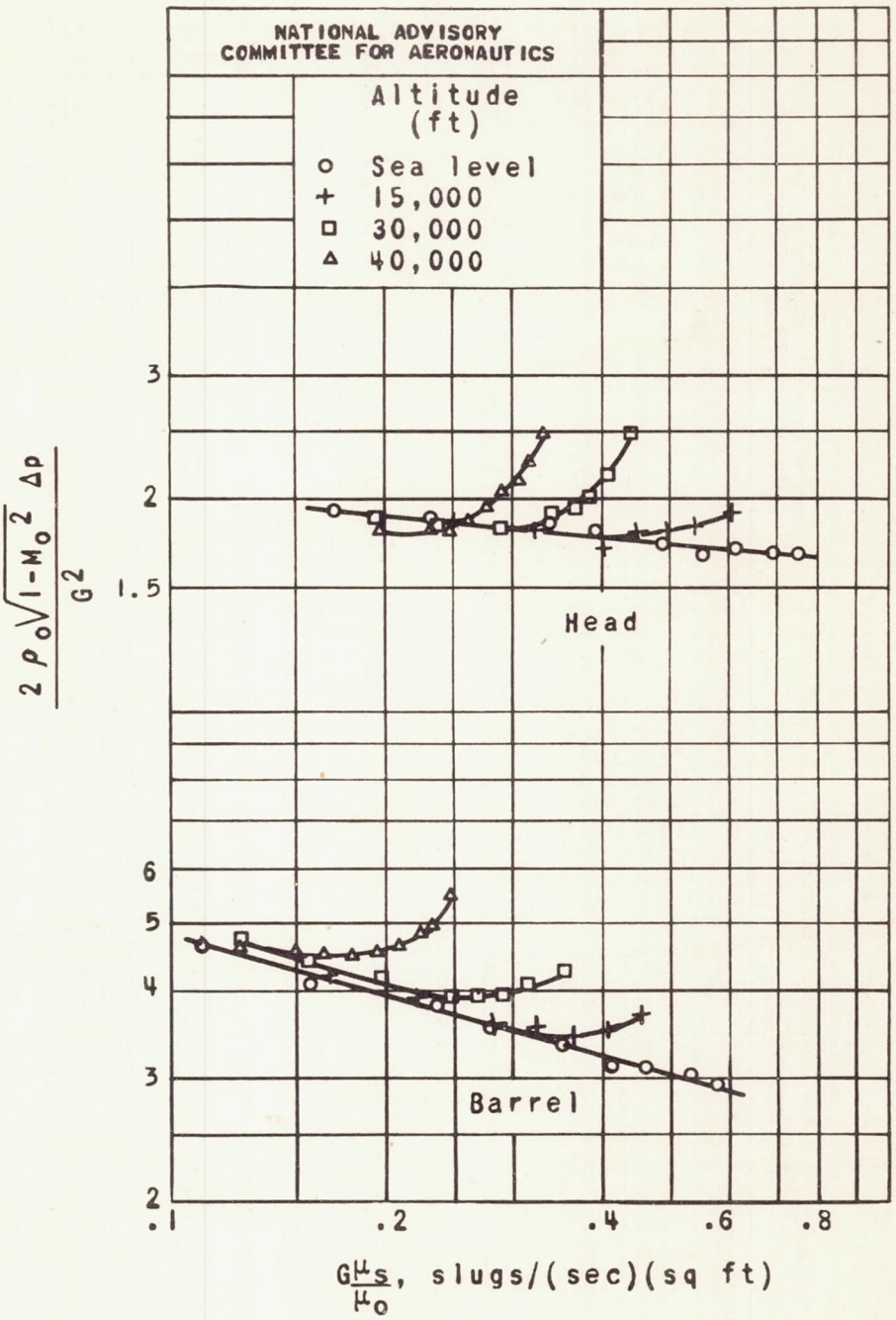
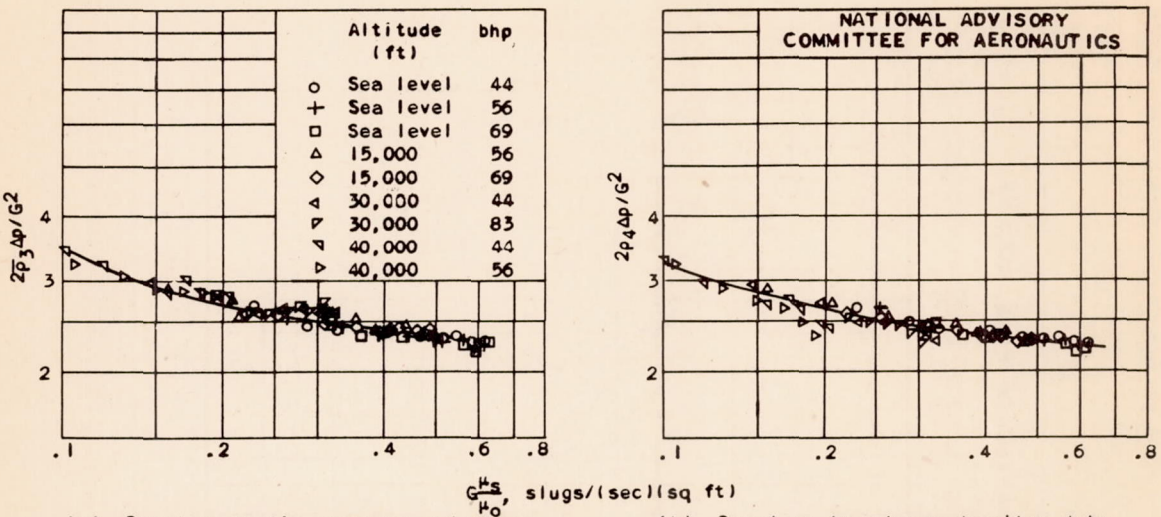
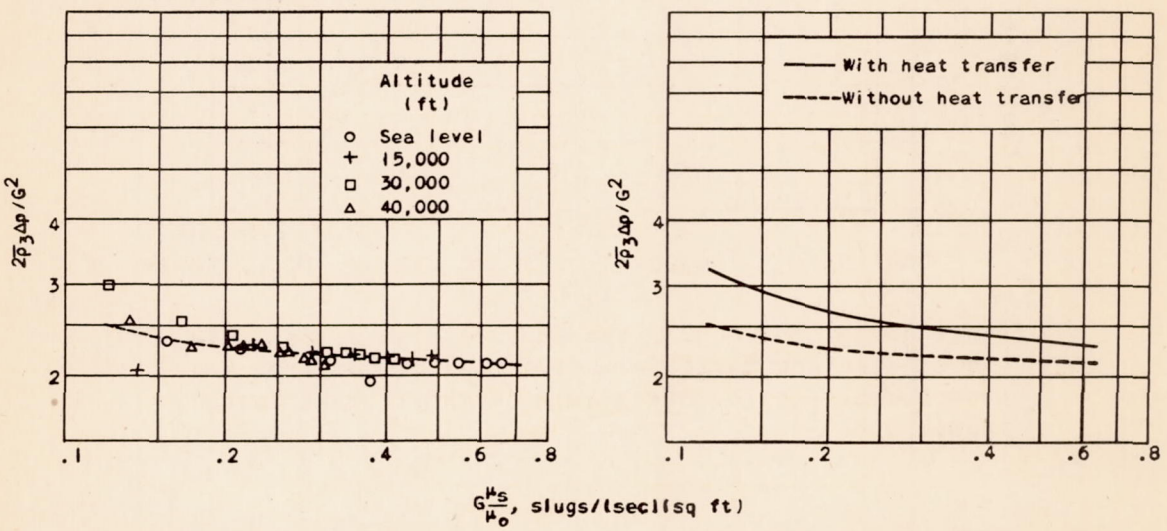


Figure 11. - Variation of pressure-loss coefficient based on characteristic Mach number with corrected mass flow of cooling air; data without heat transfer.



(a) Based on static pressure and stagnation temperature at baffle exit; data with heat transfer.

(b) Based on downstream density; data with heat transfer.



(c) Based on static pressure and stagnation temperature at baffle exit; data without heat transfer.

(d) Comparison of pressure-drop coefficients based on static pressure and stagnation temperature at baffle exit with and without heat transfer.

Figure 12. - Pressure-drop coefficients for combined head and barrel determined with and without heat transfer.

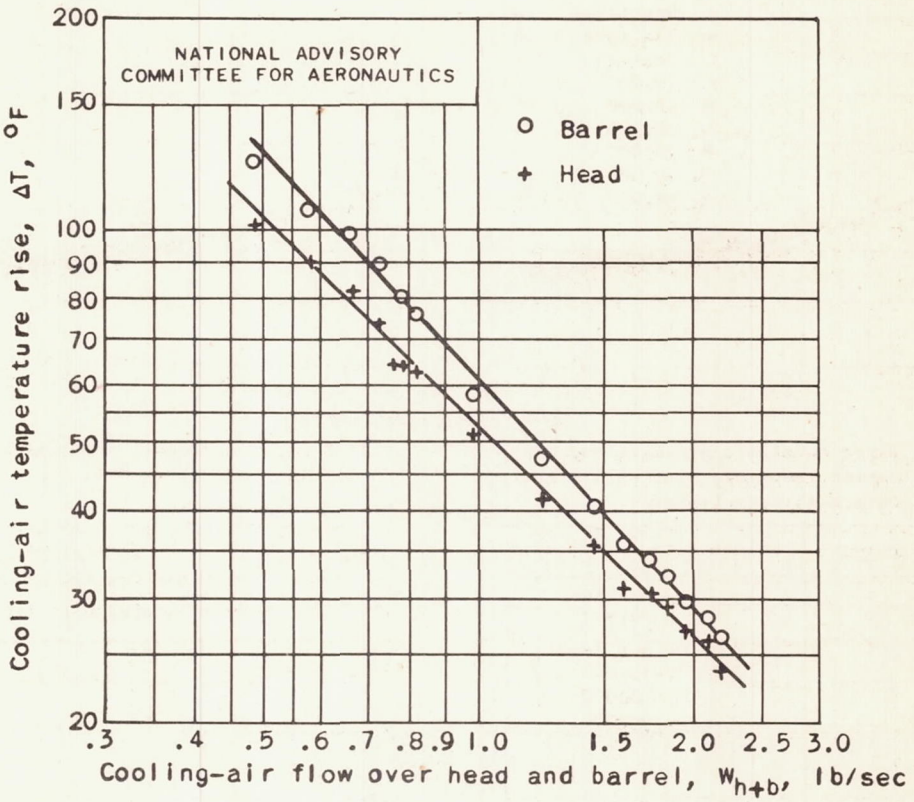


Figure 13. – Cooling-air temperature rise across cylinder head and barrel as a function of combined head and barrel cooling-air flow. Cylinder brake horsepower, 56.

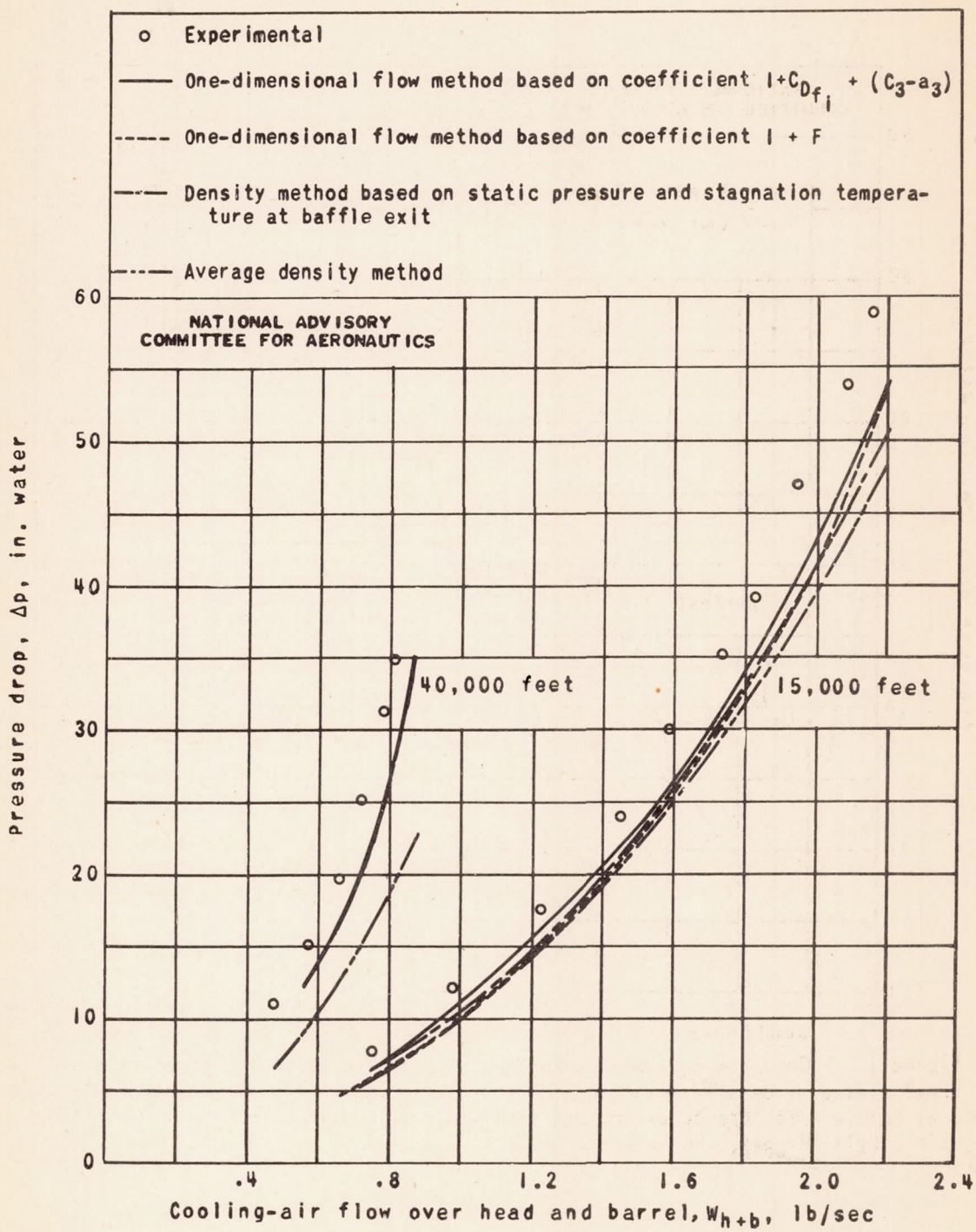


Figure 14. - Comparison between experimental and calculated pressure drops; calculations based on pressure-drop coefficients obtained from test data without heat transfer. Cylinder brake horsepower, 56.

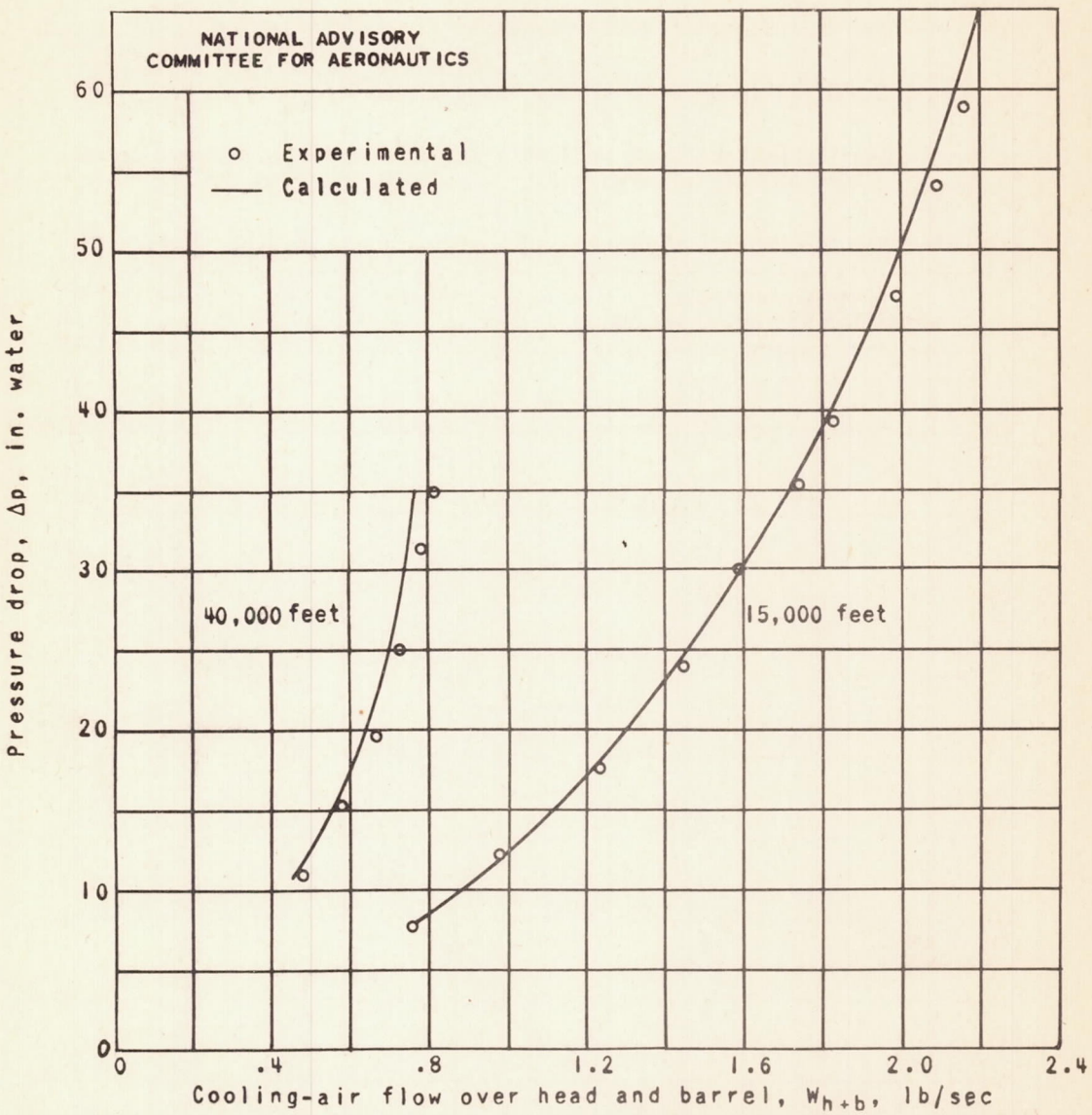


Figure 15. - Comparison between experimental pressure drops and pressure drops calculated by density method based on static pressure and stagnation temperature at baffle exit; pressure-drop coefficients obtained from tests with heat transfer. Cylinder brake horsepower, 56.